Juha Viitanen

Inverter Module Usage as a DC Power Supply for Solar Pump Application EMC Testing

Metropolia University of Applied Sciences

Bachelor of Engineering

Degree Programme in Electrical and Automation Engineering

Bachelor's Thesis

3 May 2022

Abstract

Author:	Juha Viitanen
Title:	Inverter Module Usage as a DC Power Supply for Solar Pump Application EMC Testing
Number of Pages:	47 pages
Date:	3 May 2022
Degree:	Bachelor of Engineering
Degree Programme:	Electrical and Automation Engineering
Professional Major:	Electrical Power Engineering
Supervisors:	Kari Ahlskog, Principal Engineer (ABB Oy)
	Eero Kupila, Senior Lecturer (Metropolia UAS)

This thesis work was done for ABB Oy. The purpose of the work was to find an in-house solution for solar pump EMC testing. Also, commercial DC power solution was tested. Comparison of the devices was made, and decision considering on the research results was made. The measurement results were compared to the limits defined by IEC62920 standard and the results had to be at an acceptable level.

This study was focused on the conducted emissions common mode noise. The problem with conducted emissions is increasing as components are getting smaller “the miniaturization”. The problem with the EMI is growing more serious with the component miniaturization and it has become a research focus globally.

At the beginning of the research there were two devices, provided by ABB, that were potentially promising to work as a solution to the solar pump EMC testing problem. Modules R11 and R8i were investigated, and setups were built to reduce the EMI as much as possible to get the best possible outcome from these devices.

As the result of this research, the information of the in-house solution for ABB was achieved. Even though the solution based on this works results does not come from ABB, the measurement results with the setups used gives valuable information about the usage of the device in this particular way. The measurements in the work also deepened the understanding of conducted emissions and can give to the reader valuable tools to suppress or prevent the EMI in their work.

Keywords: Variable Frequency Drive, Solar Pump application, Electromagnetic compatibility, Conducted emissions

Tiivistelmä

Tekijä:	Juha Viitanen
Otsikko:	Vaihtosuuntaajamoduulin käyttö tasavirtajännitelähteenä aurinkopumppukäyttö sovellusten EMC testauksessa
Sivumäärä:	47 sivua
Aika:	3.5.2022
Tutkinto:	Insinööri (AMK)
Tutkinto-ohjelma:	Sähkö- ja automaatiotekniikka
Ammatillinen pääaine:	Sähkövoimatekniikka
Ohjaajat:	Pääinsinööri Kari Ahlskog Lehtori Eero Kupila

Opinnäytetyö tehtiin ABB Oy:lle. Työn tarkoituksena oli löytää ABB:n laitteista ratkaisu aurinkopumppujen EMC-testaukseen. Myös kaupallista tasavirtalähdettä testattiin. Mittaustuloksia verrattiin standardin IEC62920 antamiin raja-arvoihin, ja tulosten tuli olla raja-arvojen alapuolella. Laitteita verrattiin toisiinsa ja tutkimustulosten perusteella tehtiin päätös sopivimmasta laitteesta.

Työssä keskityttiin johtuneiden emissioiden aiheuttamien vuotovirtojen mittaamiseen. Johtuneiden päästöjen ongelmat kasvavat, mitä pienemmiksi komponentit tehdään. EMI-ongelmien kasvaessa, on siitä tullut globaalisti tutkimuksen painopiste.

Työssä tarkasteltiin kahta toiminnaltaan lupaavaa ABB:n laitetta, joista voisi tulla ratkaisu aurinkopumppu sovellusten EMC-testausongelmaan. Moduuleilla R11 ja R8i tehtiin mittauksia asetelmilla, joilla EMI-vuotovirrat pyrittiin erilaisten komponenttien avulla saada mahdollisimman pieneksi.

Tutkimuksen tuloksena saatiin tietoa ABB:n omista laitteista. Vaikka ratkaisu ongelmaan ei tullut ABB:ltä, mittaukset antavat arvokasta tietoa laitteista. Työssä tehdyt mittaukset syvensivät ymmärrystä johtuvista päästöistä ja antavat lukijalle arvokasta tietoa, miten tukahduttaa tai estää EMI:tä.

Avainsanat: taajuusmuuttaja, aurinkopumppu sovellus, sähkömagneettinen yhteensopivuus, johtuvat emissiot

Contents

List of Figures

List of Tables

List of Abbreviations

AC:	Alternating Current
DC:	Direct Current
EMC:	Electromagnetic compatibility
EMI:	Electromagnetic interference
EMS:	Electromagnetic susceptibility
EUT:	Equipment Under Test
FFT:	Fast Fourier Transform
INU:	Inverter Unit
ISU:	IGBT Supply Unit
LISN:	Line Impedance Stabilization Network
PCB:	Printed Circuit Boards
PEF:	Passive EMI Filter
PWM:	Pulse Width Modulation
QP:	Quasi-Peak
RFI:	Radio Frequency interference
RMS:	Root-mean-square
VFD:	Variable Frequency Drive

1 Introduction

The main purpose of this work was to find an in-house solution for solar pump EMC testing. Because of commercial DC power supplies for EMC testing are extremely expensive, it is in the best interest for ABB to find working solution from its own existing products with some modifications to this problem. In this work it was investigated if inverter module R8i or R11 with LCL filter can act as DC power supply for solar pump EMC testing. The existing products used in the work were ACS880-104-730A inverter module configured as ISU unit with suitable setup including LCL-filter and ACS880-34-650A-3 single drive module.

The basic working principles and main differences of VFD's (Variable Frequency Drive) and Solar Pumps are presented. In addition, common usage of such power electronics conversion products is introduced. To be able to show that the developed products are in compliance with the EMC requirements, the standards play a significant role. There are several types of EMC standards for electronic and measurement equipment, which specify limits and measurement methods. In this thesis the most common drives and photovoltaic inverter related EMC standards are introduced.

EMI filtering methods were also researched, and most common methods applied in this work are passive EMI filters, shielding, cable routing and segregation. Basic EMI filter is introduced to reduce low frequency conducted emissions in common and differential modes in the frequency range 150 kHz – 30 MHz. In the measurements the state-of-the-art EMI test receiver was used with DC and AC coupling/decoupling network (also known as LISN = Line Impedance Stabilization Network). Working principle of Time Domain Scan EMI test receiver is presented, which uses FFT (Fast Fourier Transform) method to convert time domain signal to frequency domain extremely fast and reduces testing time significantly.

At the end, the different DC power source options are compared, and EMI mitigation methods presented. Also, an actual Solar Pump unit was tested against EMC standards requirements with selected and modified DC power source.

2 Variable Frequency Drive and Solar Pumps

2.1 Variable Frequency Drive Operation Principle

Variable Frequency Drive (VFD) is used to operate an AC motor with desired speed, torque, or power by changing the frequency and voltage of the fixed AC voltage from the mains. The AC motor speed depends on the number of the motor poles of the motor and the frequency of the power applied to the motor. If the output frequency is 50 Hz (main frequency used in Finland), the motor will run at its rated speed. If the frequency of the supply voltage is increased or decreased above or lower than 50 Hz the motor will run faster or slower than its rated speed. (1.)

The basic principle behind the operation of VFD is based on the rectifier, intermediate circuit, inverter, and control logic. The rectifier converts the incoming alternating current (AC) power into direct current (DC) power. Since the power from mains usually is three-phase, minimum six rectifying components are needed to rectify all power from all phases. With 6 rectifiers the term 6 pulse is used. VFD may have multiple rectifier sections. Each section has 6 rectifiers enabling VFD to be 6 pulse-, 12 pulse-, 18 pulse- or 24 pulse unit. General schematic of Variable Frequency Drive can be seen in figure 1, where the rectifier, intermediate circuit, inverter, and control logic are presented. (2.)

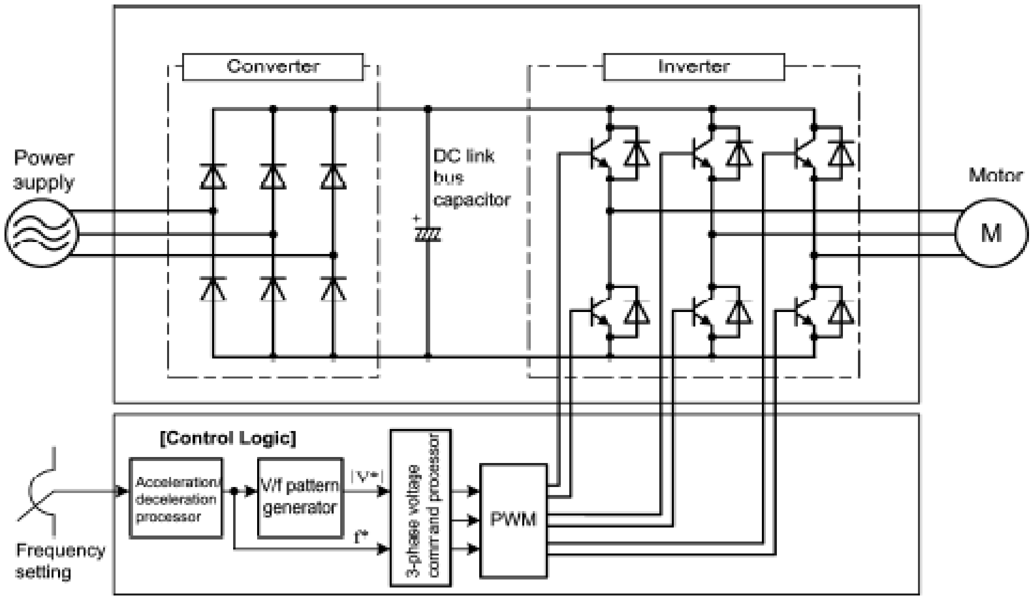

Figure 1 General schematic of VFD (3)

The rectified power is then stored at the intermediate circuit capacitors, that feeds the power further to the inverter section. To smooth the incoming power the intermediate circuit may contain chokes or inductors. (2.)

The VFD inverter section contains transistors, commonly IGBT, the "Insulated Gate Bipolar Transistors" that deliver the power to the AC motor. The purpose of the inverter section is to transform the DC voltage back to AC voltage with desired amplitude and frequency. This is done by IGBT when it uses extremely high switching frequency typically 2 to 20 kHz and switches on and off several thousands of times per second. The method is called Pulse Width Modulation (PWM). VFD that uses PWM generates in time domain pulsating sinusoidal AC output voltage. The control frequency and voltage generated with PWM method to the AC motor are extremely efficient and it provides high level of performance. The control logic of VFD is microprocessors that control the switching frequency of IGBTs that user with reference commands can control. (2.)

2.2 Solar Pump Application

Solar pump application enhances methodology of water pumping by putting the sun to work for all water pumping needs and operates without energy cost when used with solar panels. Solar pumps are used for example in agriculture e.g., to irrigate the crops, water livestock, or provide drinking water. They are widely used all around the world, especially in locations where the power of the sun can be used effectively. An example of a solar pump application system to fill the water supply for irrigating the crops is shown in figure 2. (4.)

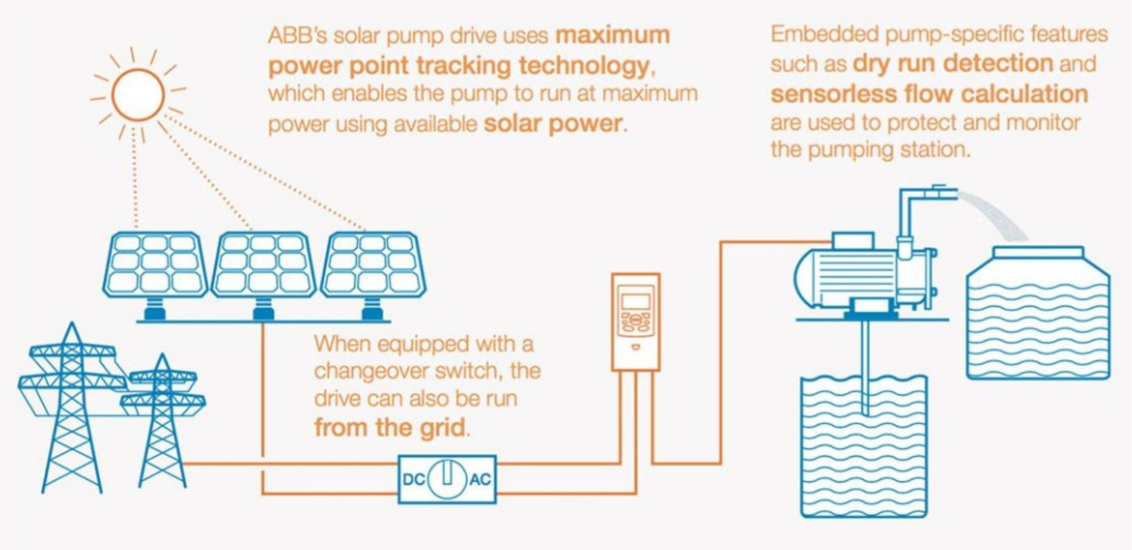

Figure 2 ABB's solar pump application example (5)

Photovoltaic Solar panel collect solar energy and convert it into DC voltage. Solar panels are connected with PV input terminals to a drive system that controls the motor of the pump. Solar pump installations are also used to manage drinking water supply, livestock watering, irrigation, and other types of residential applications. A Solar Water Pump Block Diagram that visualizes how solar intensity is used to run Solar Pump application is shown in figure 3. (6.)

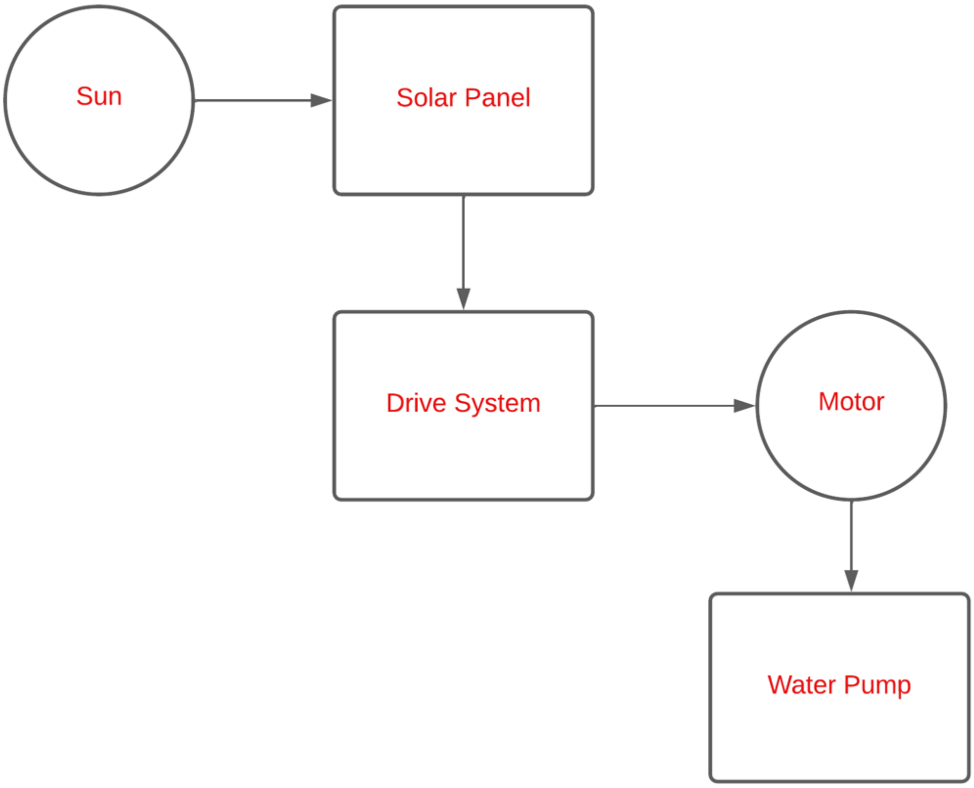

Figure 3 Solar Water Pump Block Diagram

Most of the solar pump application systems are used to control asynchronous AC induction motors or permanent magnet motors. Solar pump application drive operation principle is practically the same as VFD, only it uses the energy of the sun and converts it into electricity with DC solar panels.

Power from solar panels is fed directly to the DC bus between the rectifier and inverter, but the inverter can be also function with AC grid power source or battery. With AC grid power source, the rectifier converts alternating current and voltage into direct current and voltage. Inverter converts the direct current and voltage back to alternating current and voltage with desired frequency and amplitude. The battery uses the same power source to charge than the power fed to DC bus via PV input terminals. Battery or AC Grid Power can be also used if the load requirement is greater compared to the energy obtained by the solar panels. A block diagram of Solar Pump application where the motor of the pump can be fed with AC grid power, battery or via PV input terminals is shown in figure 4. (6.)

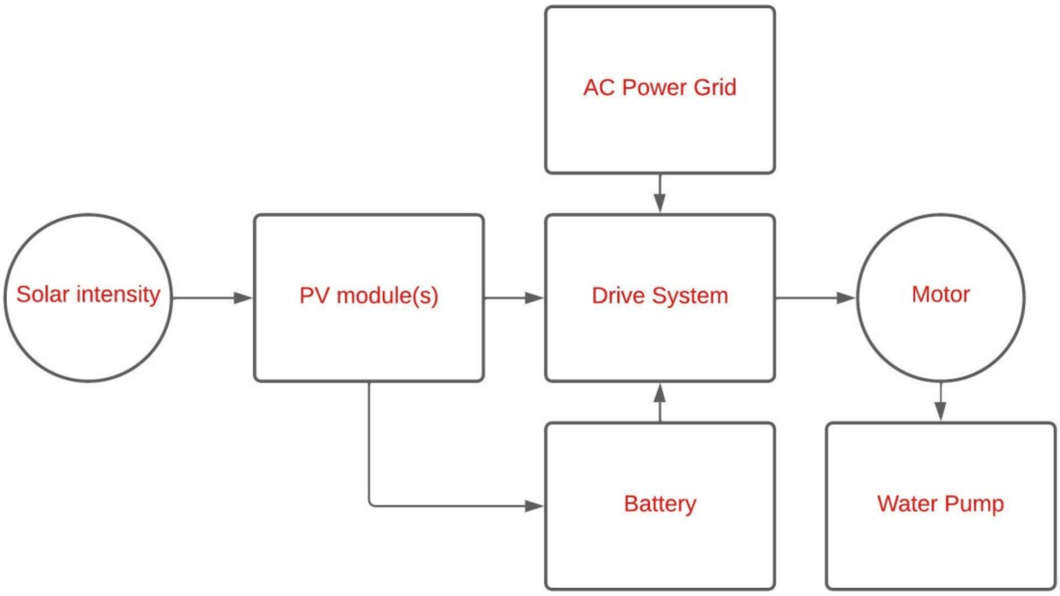

Figure 4 Solar Pump Block Diagram

PV input terminals are used to supply the DC bus of the Solar Pump Drive System. A simplified main circuit of Solar Pump application where 1. rectifier, 2. DC bus, 3. inverter, 4. and 5. PV input terminals or DC connections is shown in figure 5. (7.)

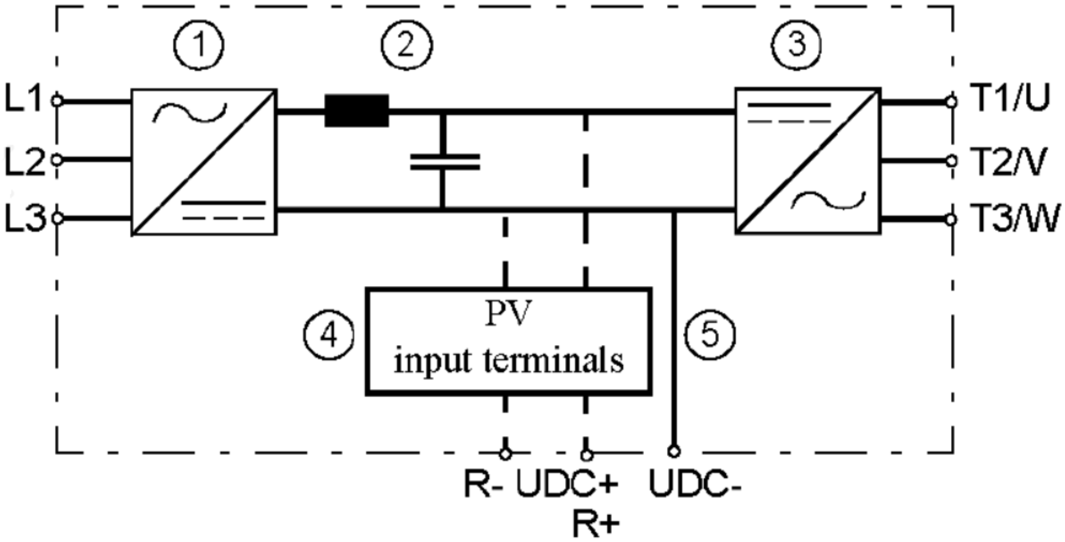

Figure 5 Simplified main circuit of Solar Pump application (7)

3 EMC

EMC stands for **E**lectro**m**agnetic **C**ompatibility. The term EMC conveys the meaning: without causing electromagnetic interference to other devices (EMI) and simultaneously being able to sustain certain level of performance defined by standards. Also, to maintain the performance level defined by standards even when exposed to electromagnetic interference from other devices (EMS). (8.)

Electronic devices tend to cause frequently radiated or conducted emissions to the surrounding environment or supply network. The term radiated emission refers to case/situation when electronic device causes unintentional release of electromagnetic energy to its surrounding environment. Radiated emissions frequency is in the range of 30 MHz to 6000 MHz. Conducted emissions are electromagnetic interference causing disturbances or “noise” via wires and PCB wiring to the supply lines. Conducted emissions frequency range is from 9 kHz to 30 MHz. Common sources of conducted emissions are electrical motor drives, switch-mode power supplies, micro-controllers, ethernet traffic, converters and appliances that are thermostatically controlled. Radiated emissions come from same sources but also from radar systems, power transmission lines, telecommunication equipment and AM/FM radio signals. (9.) A block diagram of electromagnetic coupling modes between two devices is shown in figure 6.

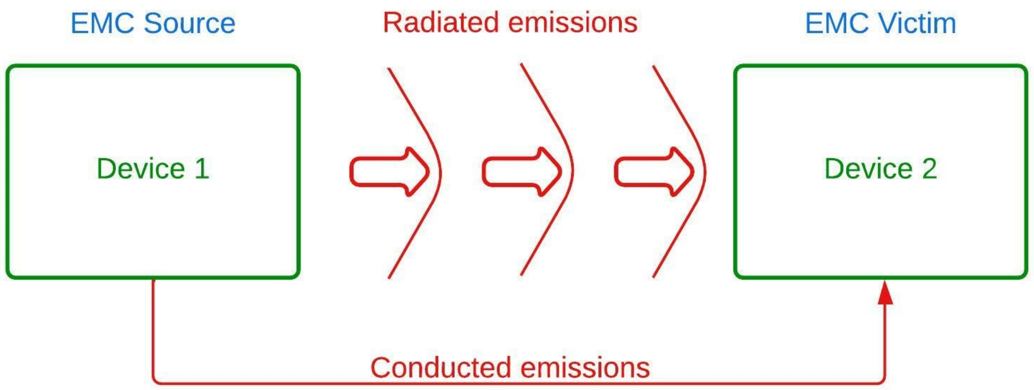

Figure 6 Block Diagram of radiated and conducted emissions between two devices

3.1 EMC Testing Principles and Conducted Emissions

EMC testing part in this Thesis focused mainly on conducted emissions. Principle of the test is the placement of the equipment under test (EUT) and line impedance stabilization network (LISN) at ground level and correct placement of the mains cable connection and the earth connections. Main point of the correct placement is to control strictly the stray coupling capacitance because it is part of the common mode circuit. The standards define the distances and lengths of the cables. (10.)

Conducted emissions are categorized in two sections: differential and common mode. Differential mode (DM) or is also called “normal mode” or “symmetrical mode” noise. Common mode noise (CM) is also called “asymmetric mode” or “ground leakage mode”. Differential Mode noise occurs in the power supply lines and the noise current flows to the same direction as the power supply current. Common mode noise current flows to the same direction in the negative and in the positive side of the circuit. It also leaks current via the stray capacitance or something similar and it passes through the ground returning to the circuit. (11.)

Common mode noise current is called “common mode” because the direction in the negative and in the positive side of the power supply is the same. (11.)

Differential mode current flows like power supply current. Outgoing and returning currents are oppositely directed and that is why it is called differential mode. In figure 7 it is shown how common mode and differential mode currents flow in a circuit.

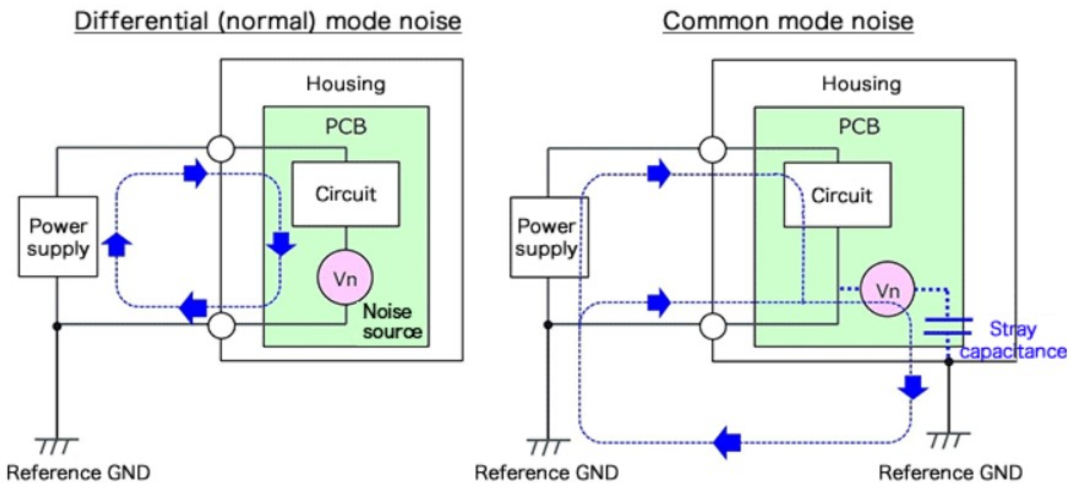

Figure 7 Differential mode and Common mode noise current flow directions (11)

3.2 EMC Standards

In this thesis two different standards define the methods and the limits of the EMC. First of the two standards is published by the International Electrotechnical Commission (IEC) and the other by International Special Committee on Radio Interference (CISPR). In this study the focus was on IEC62920 Edition 6.2 and CISRP11 Edition 1.1.
IEC62920 is a standard for Photovoltaic power generating systems – EMC requirements and test methods for power conversion equipment. CISPR is part of IEC and CISPR11 is for Industrial, scientific, and medical equipment – Radio-frequency disturbance characteristics – Limits and methods of measurement. (12; 13.)

4 EMI Filters

The high frequency switching power supply have become smaller by placing the components on PCB closer together (market requirement). This has become a problem in the performance level of the devices. The performance of electronic equipment in operation decreases the more cramped the topology in the PCB gets, thereby the problem of EMI has grown more serious. It has led to the fact that suppressing conducted EMI of switching power supply has become a subject of global research. (14.)

In figure 8 the EMI problem is being solved with EMI filter. The figure shows a typical EMI filter that is used to suppress the common mode and differential mode currents. The common- and differential mode current flow directions are presented also in the figure.

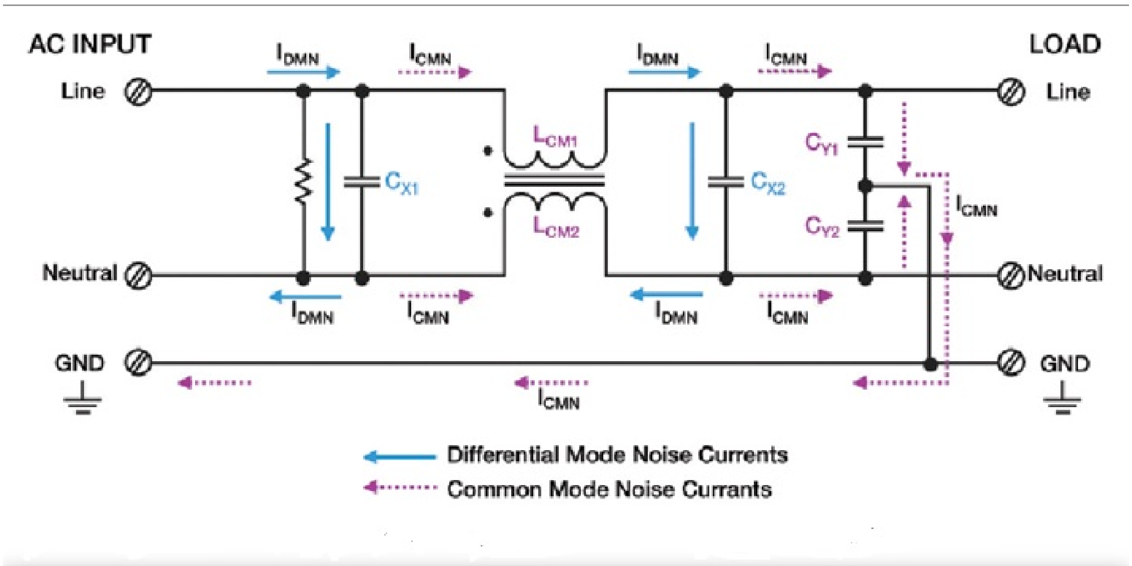

Figure 8 Typical EMI filter used to suppress the conducted EMI noise (15)

4.1 EMI Filtering Basic Principle

EMI filters or also known as RFI filters are designed to subdue or eliminate completely the noise interference generated by electronic devices. EMI filter is a device or circuit that mitigates the noise generated in the power source to its power or signal lines. This type of noise frequency range is typically from 9 kHz to 10 GHz and the effects of the noise can prevent or degrade signals or performance of the electronic device. The circuit of the typical EMI filter consists of a capacitor, inductor, and resistor. EMI filters basic operation principle is an impedance matching network. EMI filters power supply side and load side impedances are being matched inside the EMI filter circuit. The bigger the impedance adaptation is the more it attenuates the electromagnetic interference of the device. (16;17;18.)

4.1.1 Passive EMI Filter

Using PEF in a circuit is basic measure and often used technology to suppress conducted EMI. PEF has several advantages like simple design and easy installation. The biggest problem of PEF is the volume. Minimizing the volume is a bottleneck in filter development. About the small size, there is research considering for near-filed coupling to improve the filtering performance and decrease the volume of EMI filters focusing on component layout and near-field coupling. (14.)

The mostly used form of Passive EMI filter (PEF) are capacitor filter, inductance filter, and complex filter including (inverted L-type, LC filter, LCπ-type filter, and RCπ-type filter). The topologies of these filter designs are presented in figure 9. Passive filtering reduces power electronic circuits conducted emissions using inductors and capacitors to create an impedance mismatch in the EMI current path. (17.)

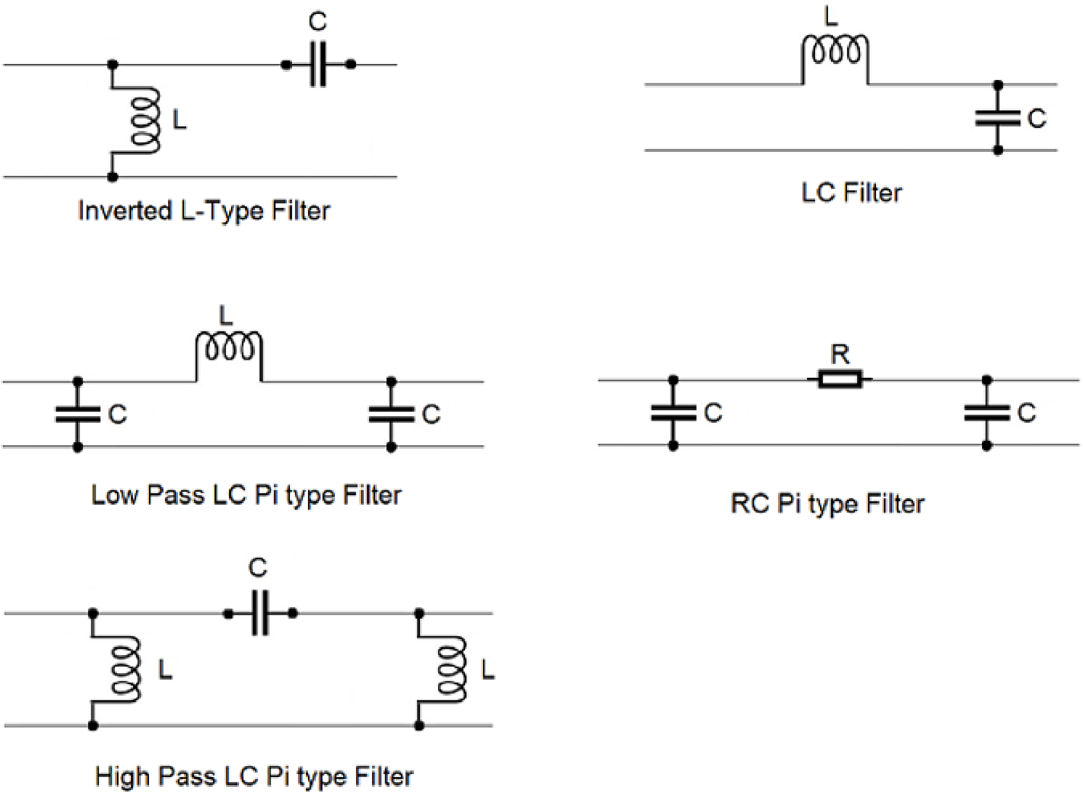

Figure 9 Topology of inverted L-type, LC filter, LCπ-type filter, and RCπ-type filter

A design of common EMI filter topology considering CM and DM noises is shown in figure 10. The EMI filter topology is mainly based on CM choke, DM capacitors and ground capacitors. Because of the CM choke, DM inductance is equivalent to the CM leakage inductance. Also, the topology of the EMI filter usually corresponds to two equivalent analysis circuits as shown in figure 11. (14.)

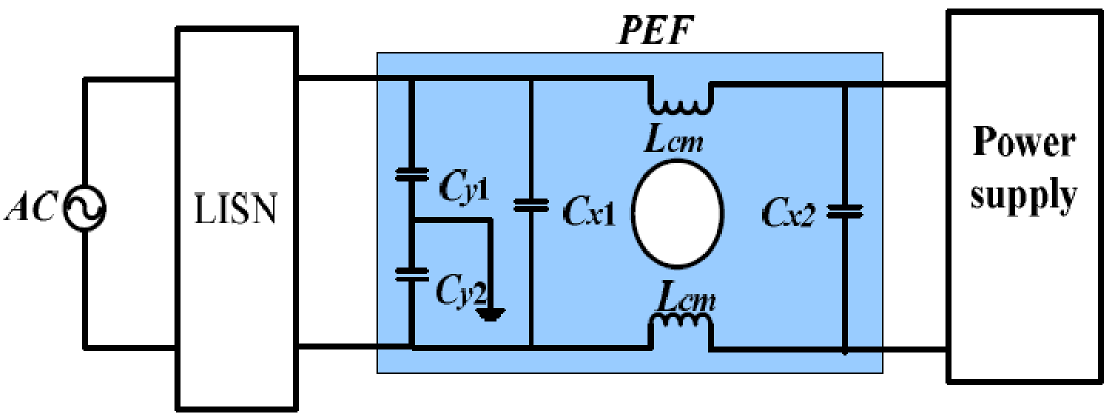

Figure 10 Usual EMI Filter topology (14)

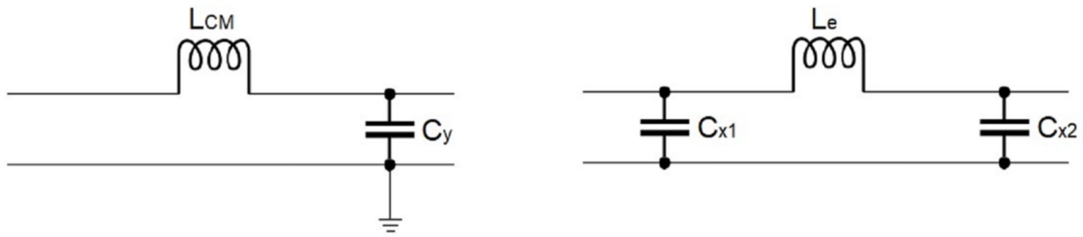

Figure 11 Two equivalent circuits. CM equivalent circuit on the left and DM equivalent circuit on the right

4.1.2 EMI Shielding

EMI shielding refers to protecting an electronic device with a metal plate or some other form of protection material from electromagnetic fields. EMI shields are designed for protecting from radiated emissions from getting through a certain point. EMI shielding is for both purposes: protection the electronic device from external radiation or prevent it emitting radiation that can cause interference to other devices. (19.)

EMI shielding reflects most of the energy of the EM wave in various directions. The wave reflects to different directions depending on the quality and material of the shielding and the phase of the wave when it hits the shield. EMI shielding also absorbs some amount of the EM wave. Absorbing the wave converts it to thermal energy and some shielding materials are made also to act as heat sinks. Depending on the heating power the device may require thermal management. (19.)

Thicker shields provide better result but also add weight to design. Most suppliers of shielding materials provide measures of effectiveness at different frequencies with the usable frequency range of the materials. These measurements help with comparing the weight and density of a shielding material to the amount of shielding it provides. Commonly used materials for EMI shielding are copper, aluminium, stainless steel, some composite materials like meshes and fabrics combined with a metal with polyester material. For shielding materials to work properly they also need good ground connections. (19.)

4.1.3 Cable Routing and Segregation

Good EMC cable routing and segregation techniques help prevent “ground loop” problems and achieve good signal quality. Installation of apparatus and their supplies should be arranged geographically to separate groups. Apparatus should be classified by voltages, high-voltage, medium voltage, and low voltage. Low voltage equipment should be also categorized as “noisy” or “sensitive”, with even more sub-categories when greater EMC control is required. (20.)

Apparatus with different classifications and their power and signal cables should be powered via different distribution networks which run separately from each other. The different classification of apparatus and their cables should be spaced well apart from each other, meters rather than centimeters. (20.)

All the current forward and return paths associated with any load should be routed closely together. Twisted pairs, triples, quads, or similar wires are best. Busbars should be spaced apart by thin layers of solid dielectric. Very heavy individual cables should be placed as close together as they can. This technique reduces both differential mode and common mode couplings, that produces magnetic and electric fields between the cable and its electromagnetic environment. (20.)

Low voltage cables ($< 1\ kV_{AC}$) are split into at least four classes, and each class run along a different route. Only cables of same class are bundled or in proximity. Cable classes would ideally not cross over each other, but where they must cross, they should do so at right angles and even then, some additional metal shielding may be required between cables more than one class apart. (20.)

5 Measuring Procedure and Devices

5.1 Measuring Devices

5.1.1 LISN, EMI Test Receiver, and Oscilloscope

Line Impedance Stabilization Network aka LISN is measuring device that is used to measure conducted emissions on power lines. LISN acts as a low-pass filter and prevents the high frequency noise of the power source. LISN provides a radio frequency (RF) noise measurement port and isolates unwanted RF signals from the power source. LISN is placed usually between the EUT and the power source. It provides a stable normalized impedance on the power input of the EUT, which is important because different power lines impedances may be very different. The EUT noise in the LISN measuring port is directly related to the impedance of the power line versus the impedance of the EUT. These two impedances create a voltage divider network for the EUT noise, allowing only small amount of noise voltage to reach to the measuring port. The reason to get reliable and consistent measuring results depends on the stable and reliable impedance LISN provide. (21.)

In this thesis work Schwarzbeck PVDC 8301 – DC-AMN LISN (figure 12) was used for measuring the disturbance voltages. A simplified circuit of the PVDC 8301 is shown in figure 13. The PVDC 8301 – DC-AMN LISN is designed specially to measure disturbance voltages at the DC-side of photovoltaic inverters. PV-inverters may cause ripple on the DC side of the inverter and may cause remarkable disturbance effects. (22.) Also, the AC side was measured with AC supply using the Schwarzbeck NNLK 8121 AC LISN to get comparable results from the AC supply side.

Figure 12 Schwarzbeck PVDC 8301 – DC-AMN LISN (23)

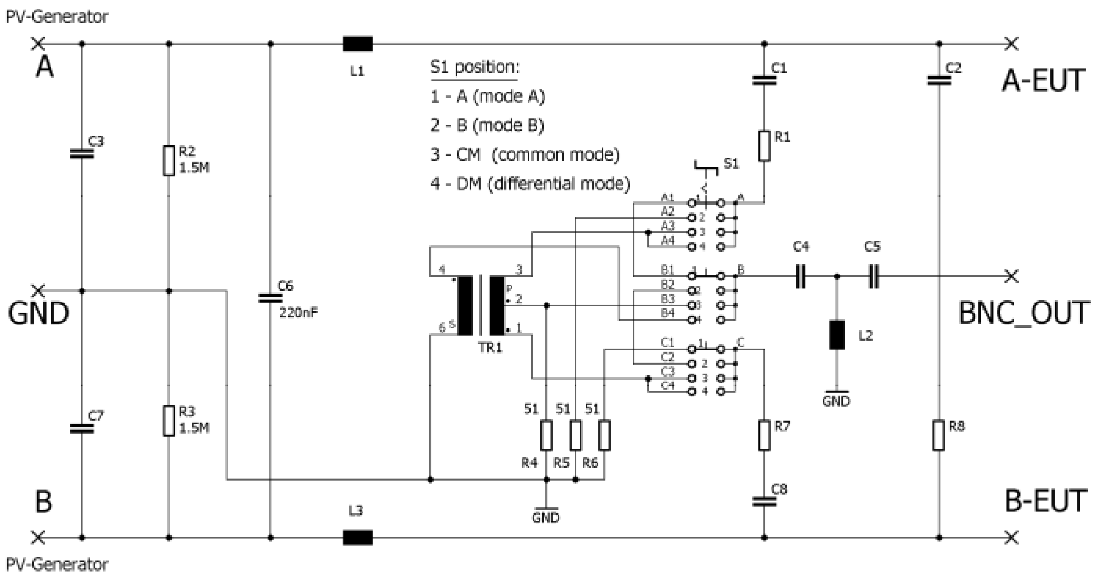

Figure 13 Simplified circuit of the PVDC 8301 (23)

In this work the Rohde & Schwarz ESPR3 (figure 14) EMI Test Receiver and signal/spectrum analyser was used. It was used to measure conducted emissions from EUT from DC couple. The frequency range ESPR3 can measure from DC couple is 9 kHz to 3.6 GHz. (24.)

Figure 14 Rohde & Schwarz ESPR3 (24)

The oscilloscope used in the work was Tektronix DPO4104 (figure 15). It was used to measure the output DC voltage from DC power source under investigation.

Figure 15 Tektronix DPO4104 (25)

5.1.2 Pulse Limiter, EMI Filter, and Other Equipment

In this work R&S ESH3-Z2 Pulse limiter (figure 16) was used to protect the EMI Test Receiver against high level RF input levels and high energy interference pulses. The Pulse limiter consists of an overvoltage arrester and a 10 dB attenuator made up of carbon-film resistors and limiter diodes with low-pass compensation. The insertion loss when Pulse limiter is connected to EMI Test Receiver is 10 dB. (26.)

Figure 16 R&S ESH3-Z2 Pulse limiter (26)

EMI filter is the basic and extremely efficient method to suppress the conducted emissions. In this work two different EMI filters were used in the measurements. The EMI filters used in setups were Schaffner EMC/EMI Filters for PV Inverters models were FN2200-75-34, FN2200-50-34, and FN2200-25-33. In figure 17 is shown a picture of Schaffner EMC/EMI FN2200-model filter. In figure 18 is shown a typical schematic of the electrical circuit of the FN2200-model.

Figure 17 Schaffner FN2200-model EMC/EMI filter (27)

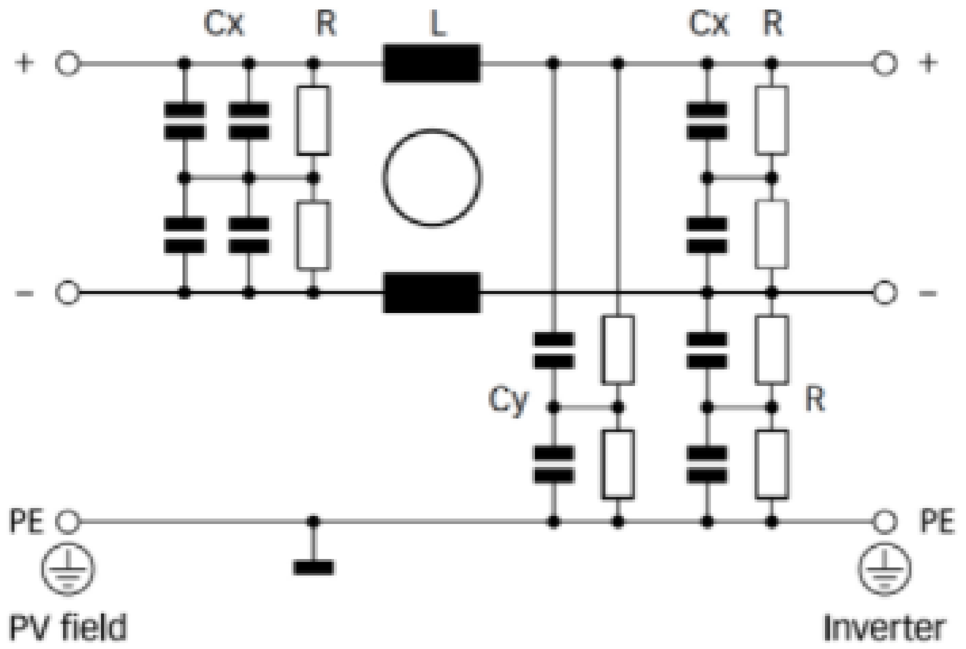

Figure 18 Schaffner FN2200-models typical electrical schematic (27)

The measurement cable used between LISN, and EMI test receiver was a coaxial cable, RG_223_U, 5 meter long with 50-ohm impedance. DC blocking diodes MDD26-12N1B. Voltage probe that was used to measure the EUT DC output voltage was Yokogawa 700924 differential probe 1400 V / 100 MHz. Schwarzbeck TK 9422 high voltage probe (9 kHz) 150 kHz – 30 MHz was used to protect the EMI test receiver in the beginning of both measurements with R11 and R8i. Motor used in the measurements was ABB M2AA 160 M 3GAA162111-ADA 3-phase squirrel cage motor. The motor was run with following specification:

-690 V Y, 50 Hz, 11,0 kW, 1460 rpm, 12,7 A, cosφ 0,81

5.2 Equipment Under Test

5.2.1 ACS880-104 – R8i

Equipment Under Test, or simply EUT in this work were ACS880-104-730A Inverter module configured as an ISU unit, with appropriate filter module BLCL 15-5, and suitable supply cabinet ISU selection 1xR8i ISU 690 V. This system was configured to operate with 500 V_{AC} supply voltage from 690 V_{AC}, by modifying the auxiliary voltage transformer.

The control program of the drive limits the minimum and maximum intermediate circuit voltages. The program with normal rating database values, limits the minimum intermediate circuit voltage to $\sqrt{2} \times U_{AC} \times (1.03 \ldots 1.08)$. With this setup the minimum DC voltage in the intermediate circuit was approximately 718 V_{dc}. The control program limits the maximum DC voltage to 799 V_{dc} with 500 V_{AC} supply. In figure 19 is shown a simplified main circuit diagram of the ACS880-104 rectifier.

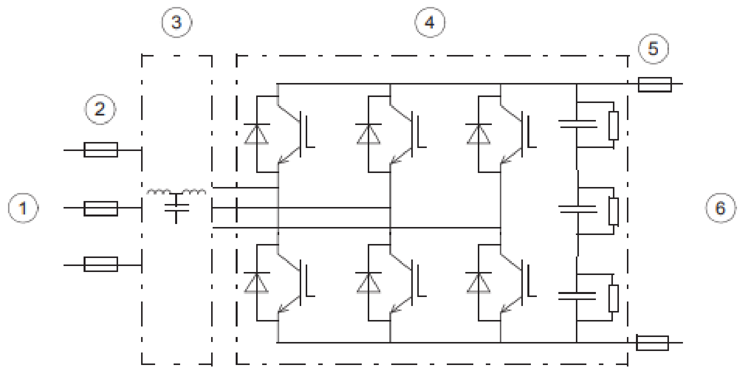

1.	AC voltage
2.	AC fuses
3.	LCL filter
4.	IGBT supply module
5.	DC fuses
6.	DC voltage

Figure 19 Simplified main circuit diagram of the ACS880-104 rectifier (28)

5.2.2 ACS880-34-503A-5 – R11

The module type used was QPU-C1-11030-5 with QLCL-15-5. This module can be configured as 503A-5 or 605A-3 device. In this work the module was configured as 503A-5 because the supply voltage parameter of the module could be easily changed from ISU control panel and simply switching the supply voltage between 400 V_{AC} and 500 V_{AC}. This allowed the rather quick changing of the voltage levels in the measurements between 400 V_{AC} and 500 V_{AC} supplies. With this module the control program of the drive limits the minimum and maximum intermediate circuit voltages. Minimum voltage in intermediate circuit is $\sqrt{2} \times U_{AC} \times (1.03\ldots1.08) = 580\ V_{dc}$ with 400 V_{AC} supply. The program limits the maximum voltage to 799 V_{dc} with 500 V_{AC} supply. The maximum voltage was used with 500 V_{AC} supply, so the measurement results between EUT would be comparable. In figure 20 is shown a block diagram of the main circuit of the ACS880-34 drive module.

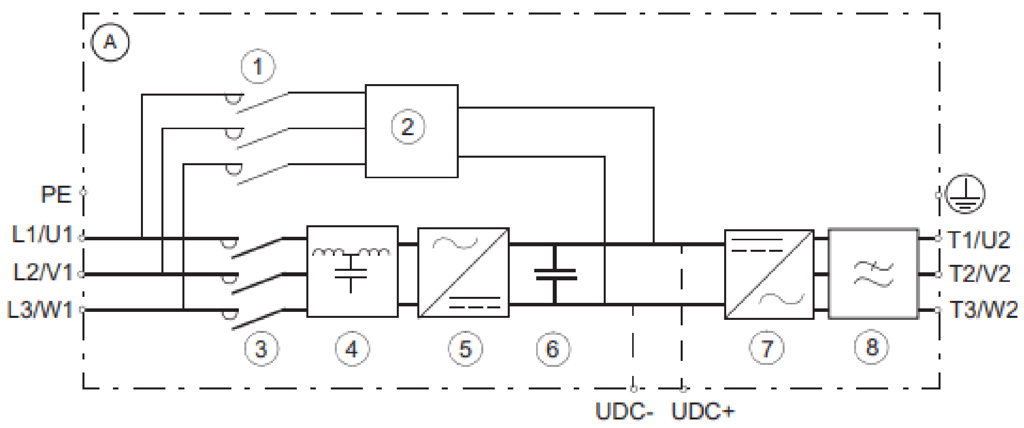

A	ACS880-34 drive module
1	Charging circuit contactor
2	Charging circuit
3	Line contactor
4	LCL filter
5	Line-side converter
6	DC link. DC circuit between the line-side converter and motor-side converter.
7	Motor-side converter
8	Common mode filter (+E208)

Figure 20 A block diagram of the main circuit of the ACS880-34 drive module (29)

5.2.3 Magna-Power

Commercial Magna-Power used in measurements to be compared to VFD's measurement results was Magna-Power model TS1000-10. It provides 0 V_{dc} to

1000 V_{dc} adjustable voltage and 10 kW power. It is light, small, and very simple to use.

5.3 Testing Laboratory and Setups

The testing laboratory was EMC laboratory in ABB facility. The laboratory is designed to have less disturbances by having its own transformer with TN-S supply network. The floor of the laboratory testing area is metal surfaced and conductive. Changing of the supply voltage manually 400 V_{AC}, 500 V_{AC} or 690 V_{AC} from the supply transformer is very easy and quickly done from control panel of the power supply. The voltage for the R11 and R8i test setups was taken with 64A sockets from the laboratories supply network. The supply voltage for the AC-LISN was taken with 32 A socket. The EMC testing laboratory meets the EMC requirements of the power drive systems by the IEC 61800-3:2017 standard what is appropriate testing conditions for the measurements of this thesis work.

5.3.1 ACS880-104 / R8i

R8i module itself cannot be operated alone as a drive. The module required a cabinet solution to operate. The cabinet provides among other things the charging circuit, LCL-filter, and busbar connections for the module to the AC supply and to the DC link. The cabin itself was only the ISU side of the whole cabin so it was conveniently open from the side that allowed access directly to the DC link as can be seen in figure 21.

Figure 21 Supply cabinet ISU selection 1xR8i ISU

The setups for testing the R8i module is presented with a block diagram below. In figure 22 is shown the first block diagram of the EUT. The EUT or the tested power source is connected to the DC-LISN with HV probes. The EUT was tested with multiple measurements by changing the placement of the HV probes.

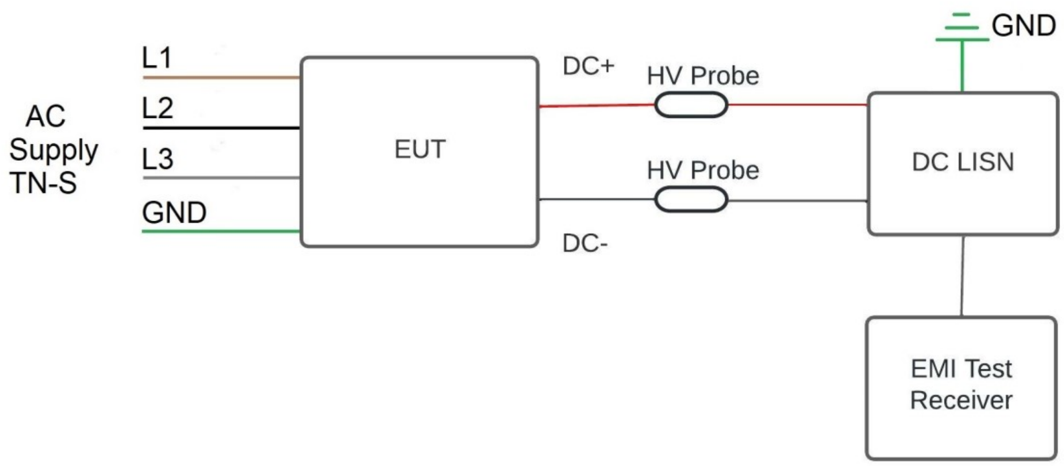

Figure 22 R8i module measurement setup presented in block diagram

In figure 23 the second setup of the R8i is presented with block diagram. MEMI-01 Filter is added to the setup to suppress the conducted emissions.

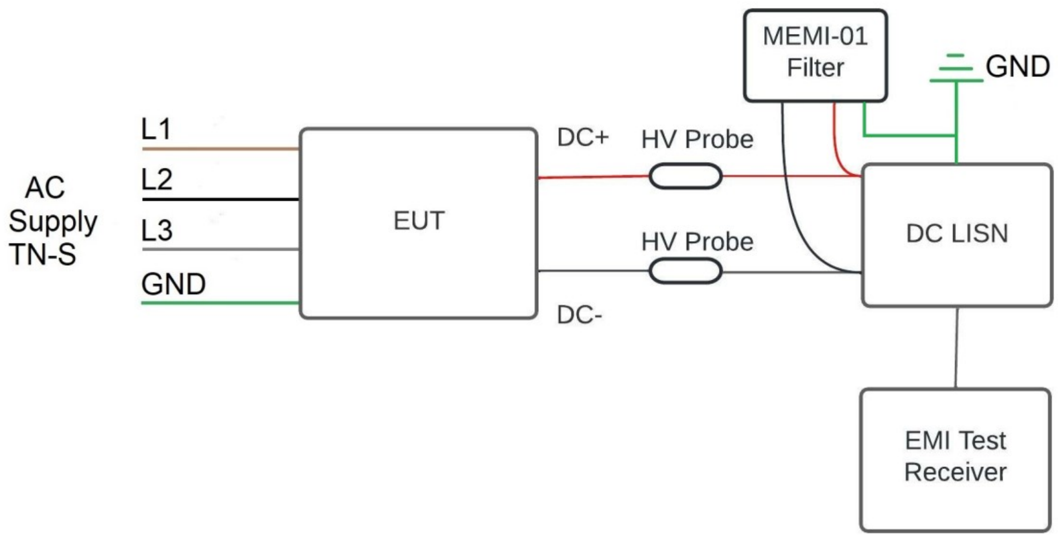

Figure 23 R8i measurment setup with MEMI-01 Filter

5.3.2 ACS880-34-503A-5 / R11

Three different block diagrams are presented in this Thesis from R11 measurement setups. First setup of R11 is presented in figure 24. It consists of

EUT (R11 the power source) which gets its supply voltage from EMC laboratory supply transformer of 400 V_{AC} or 500 V_{AC}, EMI filter, different size of capacitors in different coupling arrangement, but mostly two capacitors in cascade connection, DC-LISN, and EMI test receiver. The purpose of changing different size of capacitors was to reduce the conducted emissions as much as possible.

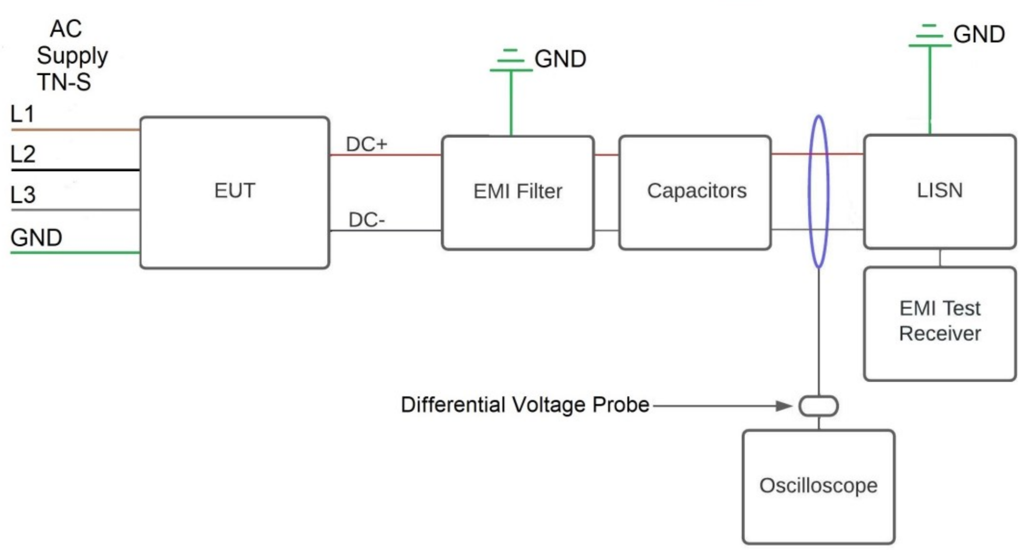

Figure 24 Measurement setup 1 of R11

Two of the setups consists of EUT (R11 the power source) with supply voltage of 400 V_{AC} or 500 V_{AC}, EMI filters, MEMI-01 filter, DC Choke, LISN, EMI test receiver, oscilloscope, DC blocking diodes, varistors and Solar Pump application connected to AC induction motor. The two setup cases (setup 2 and 3) differ only from each other when the EMI filter close to EUT is either grounded to the EUT or to the test laboratory floor. These two setups were presented for the reason that the conducted noise level with these setups were below the IEC62920 standard. In both cases the result of the EMI noise was acceptable for using the R11 as a DC power source in Solar Pump application conducted emission measurements.

The only difference on the second and on the third setup presented with block diagrams is the grounding of the EMI filter. The second setup of R11 is presented with block diagram in figure 25. The EMI filter is grounded on laboratory floor.

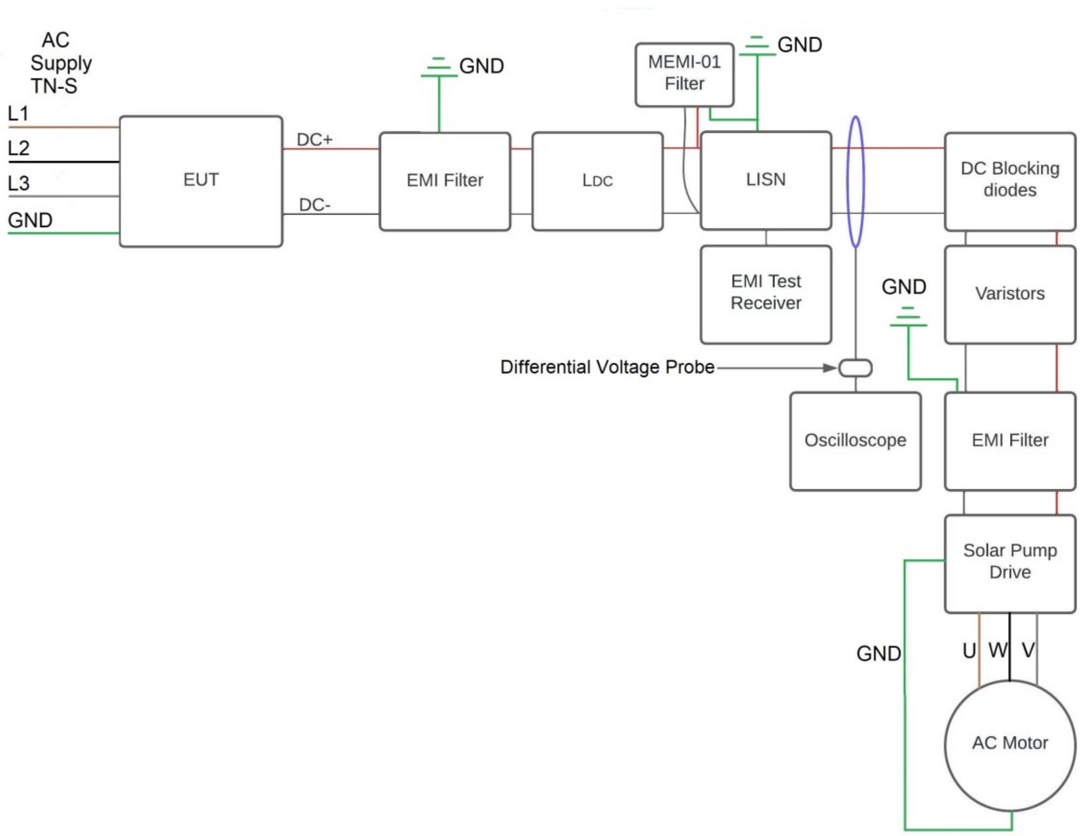

Figure 25 Setup 2 with R11 module, EMI filter grounded to laboratory floor

Third setup of R11 is presented with block diagram in figure 26. The EMI filter is grounded to the EUT. With the small grounding change, the effect of reducing the conducted noise was significant enough to present both setups and the difference between the results of the measurements which can be found later in the measurement results.

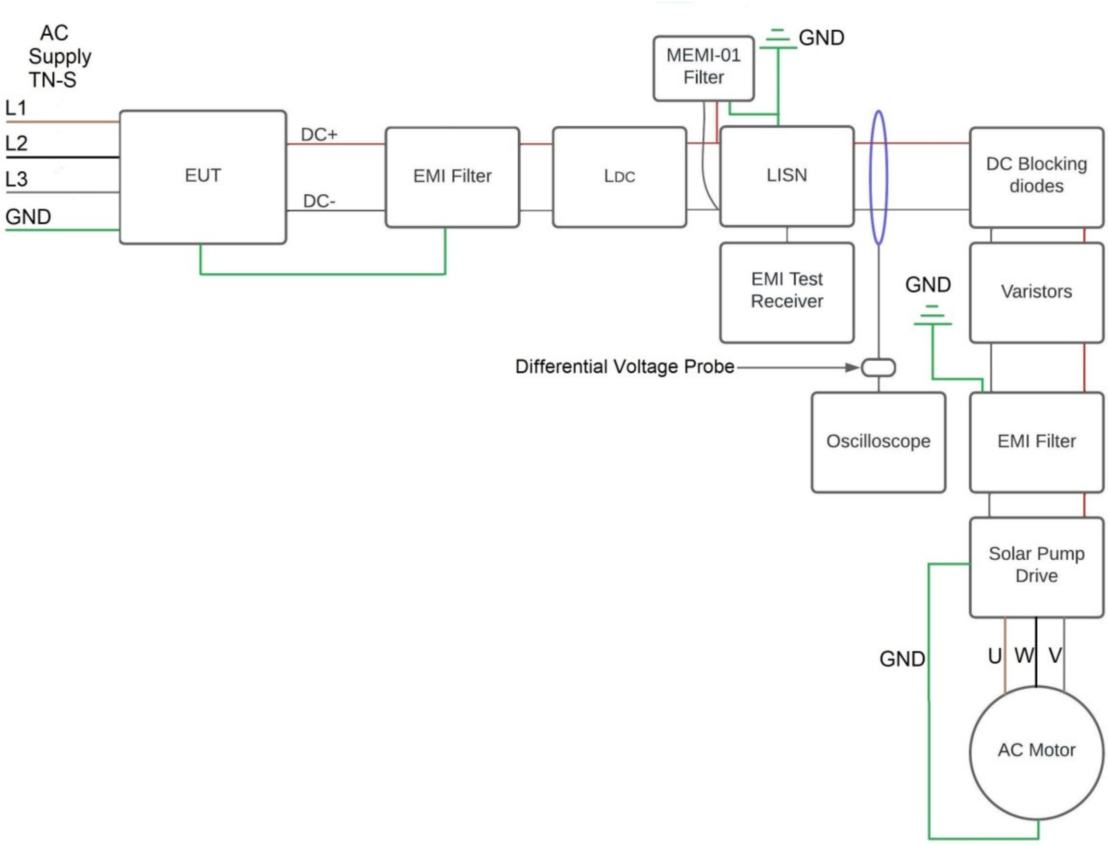

Figure 26 Setup 3 with R11, EMI filter grounded to the EUT

5.3.3 Magna-Power TS1000-10 and AC Grid Supply

Solar Pump application was tested with two different voltage supply, AC grid voltage supply and with the EUT, Magna-Power acted in this case as DC voltage supply. Solar Pump application was also tested when both supplies are applying power to the Solar Pump application simultaneously. The measurement setup is presented with block diagram in figure 27. When power supplies were tested alone the supply cables from another supply was disconnected during the measurements.

Magna-power supply voltage is taken from EMC laboratory supply transformer (400 V_{AC}) with 32 A socket. Rest of the Magna-power measurements setup includes EMI filters, MEMI-01 filter, LISN, EMI test receiver, DC blocking diodes, varistors and Solar Pump application connected to AC induction motor. AC grid voltage is taken 400 V_{AC} supply with 32 A socket. The AC grid voltage goes only through LISN to the Solar Pump application.

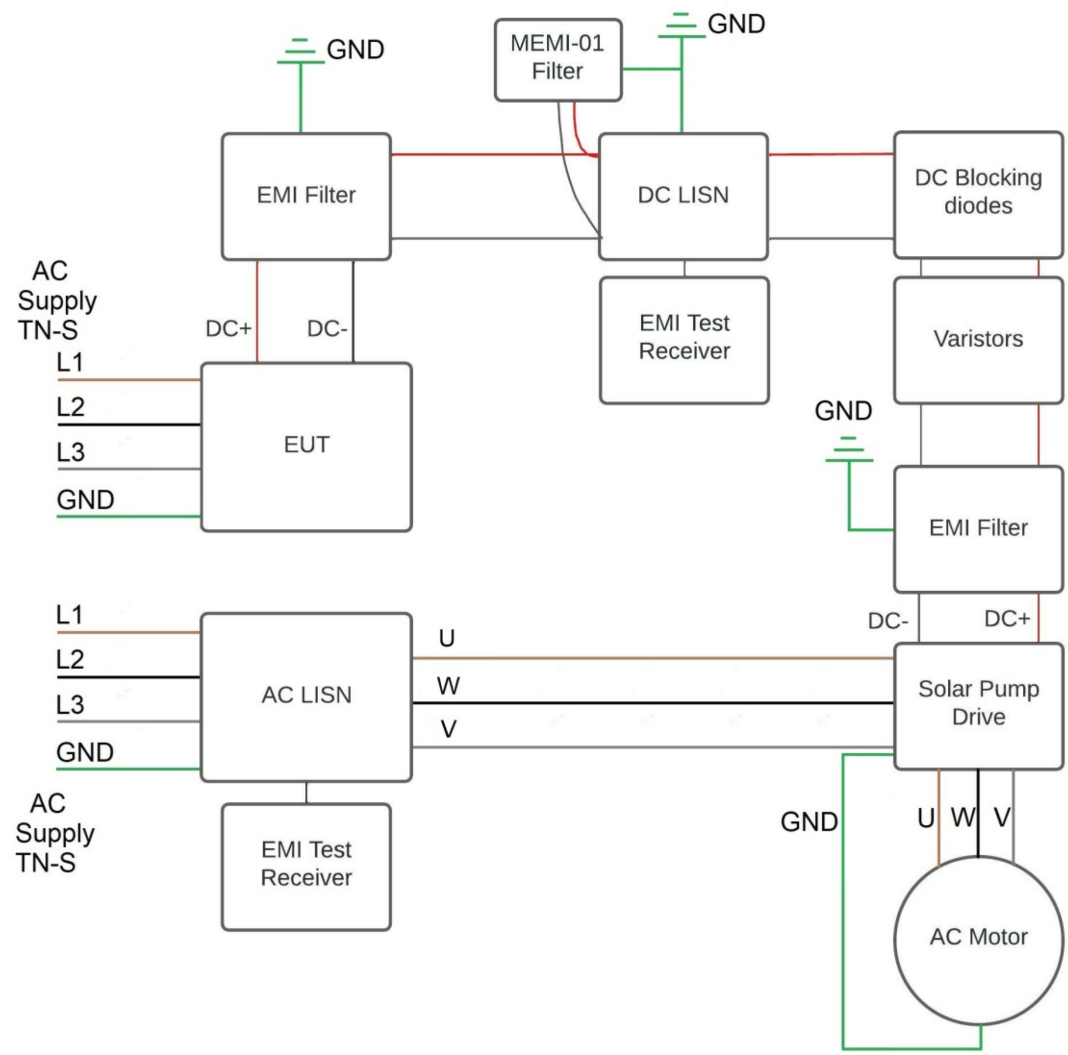

Figure 27 Magna-Power and AC grid supply setup block diagram

6 Measurement Results

The purpose of the thesis work was to find a power source that can be used to test the conducted emissions from Solar Pump application. The wanted result of the power source was that the noise levels of the EUT (power source) would stay under the limits of the standard IEC62920 in which the measurement results were compared. The worst-case scenario on conducted emissions are the common mode currents that are presented mostly in the measurement results, because they define the conclusion about the apparatus. The standards define the noise levels of the measurements. Table 1 below shows maximum noise level (ripple voltage) for DC-Power supply in the frequency range 150 kHz – 30 MHz with device rated power of ≤ 20 kVA and table 2 with the device rated power of ≥ 20 kVA.

Table 1 Maximum noise level (ripple voltage) for DC-Power supply in the frequency range 150 kHz – 30 MHz with device rated power of ≤ 20 kVA

f [MHz]	QP [dBµV] IEC62920	6dB Margin [dBµV]
0.15	97	91
5	89	83
30	89	83

Table 2 Maximum noise level (ripple voltage) for DC-Power supply in the frequency range 150 kHz – 30 MHz with device rated power of ≥ 20 kVA

f [MHz]	QP [dBµV] IEC62920	6dB Margin [dBµV]
0.15	116	110
5	106	100
30	89	83

Table 3 below shows maximum noise level (ripple voltage) for AC mains power supply in the frequency range 150 kHz – 30 MHz with device rated power of ≥ 20 kVA.

Table 3 Maximum noise level (ripple voltage) for AC-Power supply in the frequency range 150 kHz – 30 MHz with device rated power of ≥ 20 kVA

f [MHz]	QP [dBµV] IEC62920	6dB Margin [dBµV]
0.15	100	94
5	86	80
30	73	67

Quasi-peak limit IEC62920 class A rated power of ≤ 20 kVA [dBµV] with DC-LISN is shown in figure 28, and quasi-peak limit IEC62920 class A rated power of ≥ 20 kVA [dBµV] with DC-LISN is shown in figure 29. Graphs are presented in values as a function of amplitude (dBµV) and frequency (Hz).

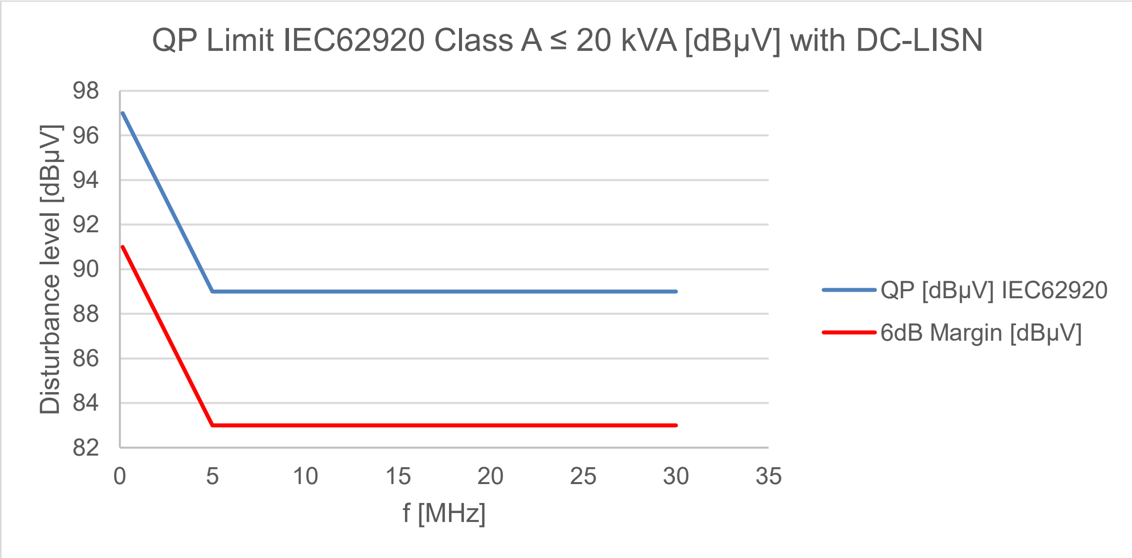

Figure 28 Quasi-Peak Limit IEC62920 Class A ≤ 20 kVA [dBµV] with DC-LISN

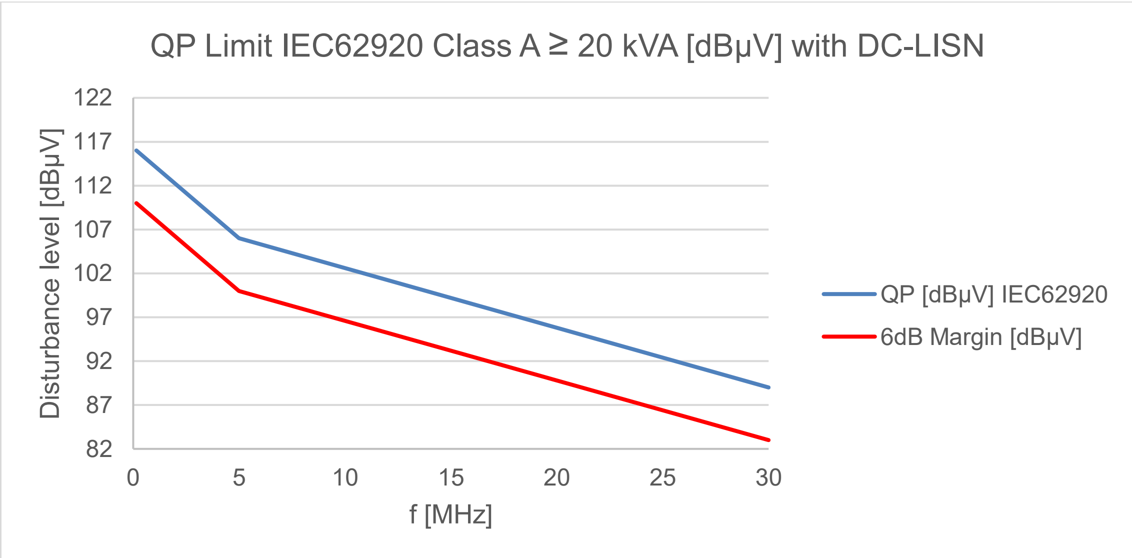

Figure 29 Quasi-Peak Limit IEC62920 Class A ≥ 20 kVA [dBµV] with DC-LISN

Quasi-peak limit IEC62920 class A ≥ 20 kVA [dBµV] with DC-LISN in values as a function of amplitude (dBµV) and frequency (Hz) is shown in figure 30.

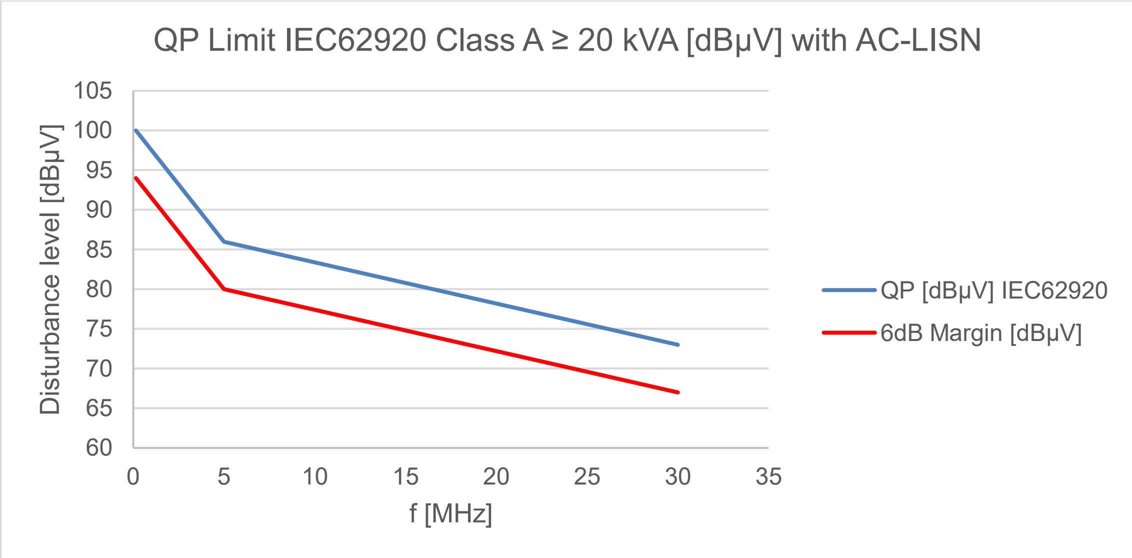

Figure 30 Quasi-Peak Limit IEC62920 Class A ≥ 20 kVA [dBµV] with AC-LISN

6.1 Measurement Results of R8i

Measurement comparison of R8i quasi-peak is shown in figure 31 using Schwarzbeck TK 9422 HV probes. Measurements M1 and M3 are taken from DC+ busbar from the EUT's DC link in which case the impedance is unknown. Measurement M5 is taken thru DC-LISN, and impedance is known. Voltage is 718 V_{dc} with measurements M1 and M5. Voltage with measurement M3 is 799 V_{dc}. IEC62920 limit class A rated power of ≤ 20 kVA is used as a measurement comparison in the graph. Setups used in measurements are presented in chapter 5.3.1.

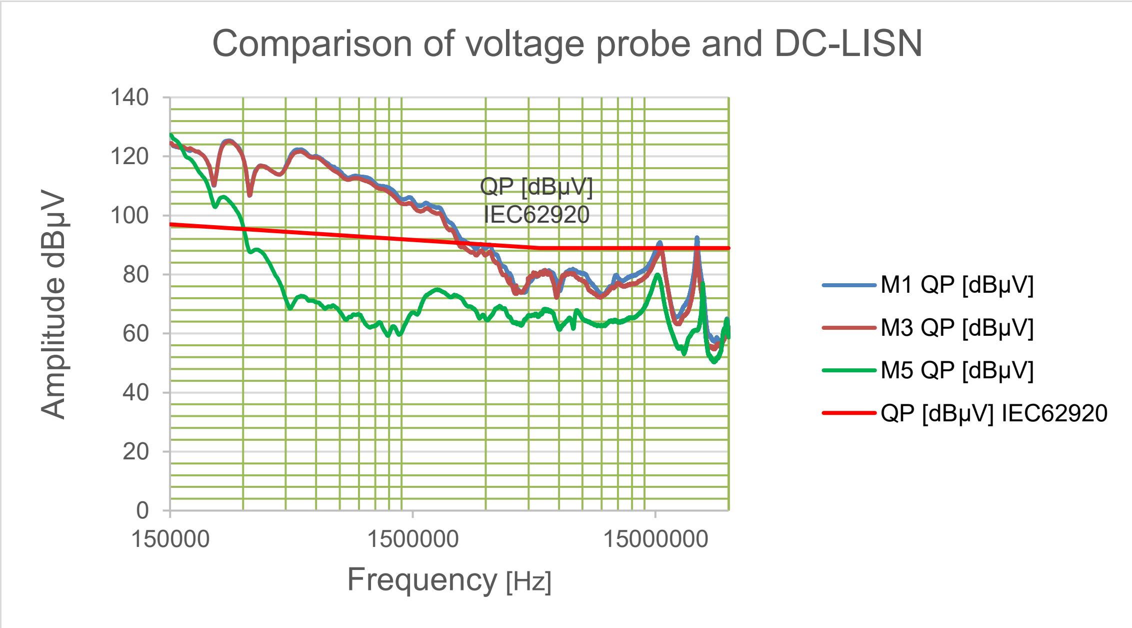

Figure 31 Measurements of R8i known impedance vs. unknown impedance

A measurement comparison of R8i when LISN is set to measure common mode quasi-peaks with 718 V_{dc} is shown in figure 32. Measurement M17 is taken thru DC-LISN, reference measurement. Measurement M21 is taken thru DC-LISN, and MEMI-01 filter has been added to the setup. IEC62920 limit class A rated power of ≤ 20 kVA is used as a measurement comparison in the graph.

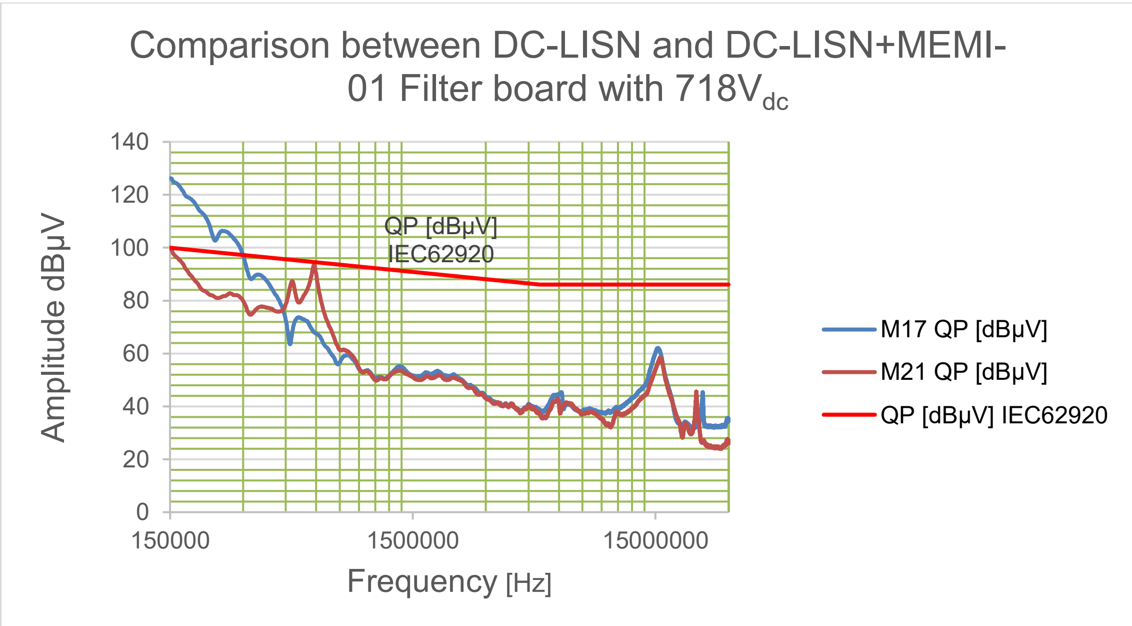

Figure 32 Measurement of R8i common mode quasi-peaks with 718 V_{dc}

A measurement comparison of R8i when LISN is set to measure common mode quasi-peaks with 799 V_{dc} is shown in figure 33. Measurement M19 is taken thru DC-LISN, reference measurement. Measurement M23 is taken thru DC-LISN, and MEMI-01 filter has been added to the setup. IEC62920 limit class A rated power of ≤ 20 kVA is used as a measurement comparison in the graph.

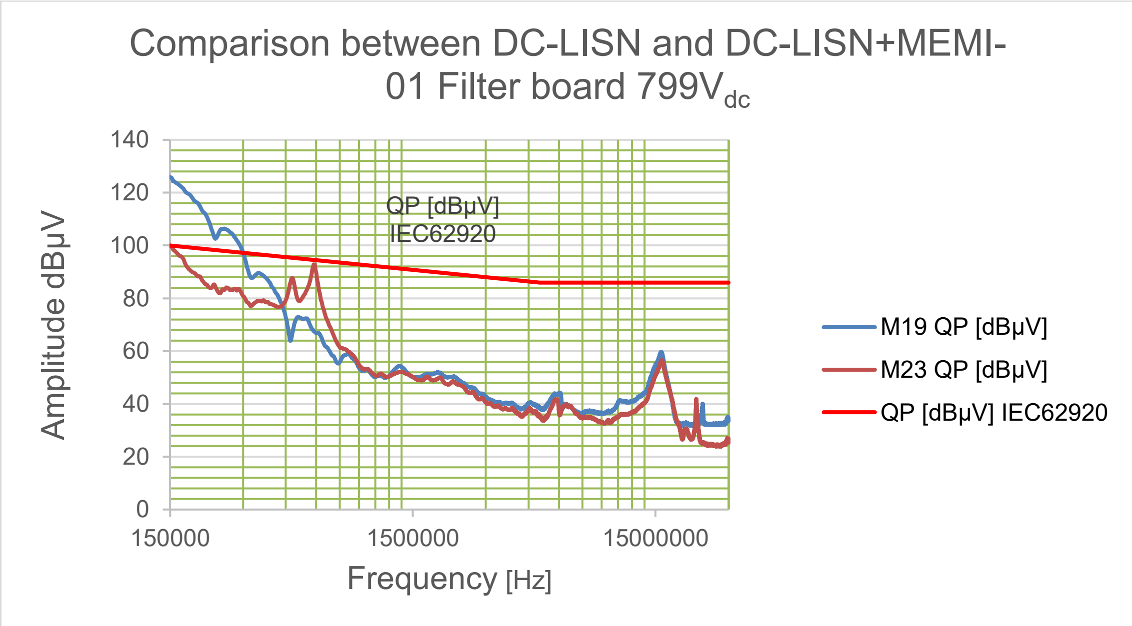

Figure 33 Measurement of R8i common mode quasi-peaks with 799 V_{dc}

In table 4 is shown the maximum quasi-peak values from all the measurements presented in this thesis from the R8i.

Table 4 Maximum quasi-peak values from measurements with R8i

Measurement case	Quasi-peak maximum value between range of 0.15 – 30 MHz
M5	127.34 dBµV
M17	126.31 dBµV
M19	125.87 dBµV
M21	99.67 dBµV
M23	99.82 dBµV

6.2 Measurement Results of R11

Comparison of three different measurement results when voltage reference is set to 580 V_{dc} is shown in figure 34. Measurements are quasi-peak values as a function of amplitude (dBμV) and frequency (Hz). In the measurement M1, the EUT is connected only to the DC-LISN, reference measurement. In the measurement M5, the EUT is connected to the DC-LISN and EMI filter Schaffner FN2200-75-34 (1200 Vdc, 75 A) is added to the setup. In the measurement M9, the EUT is connected to the DC-LISN with EMI filter Schaffner FN2200-75-34, and between the drive and DC-LISN is added 2 x 1.5 μF capacitors in series from +/- to reference ground plane (between EMI filter and DC-LISN). IEC62920 QP limit class A rated power of ≤ 20 kVA is used as a measurement comparison in the graph. The measurement setup is presented in chapter 5.3.2. The graph itself tells that more modification to the setup is needed to reduce the conducted emissions to the accepted level by the standard IEC62920.

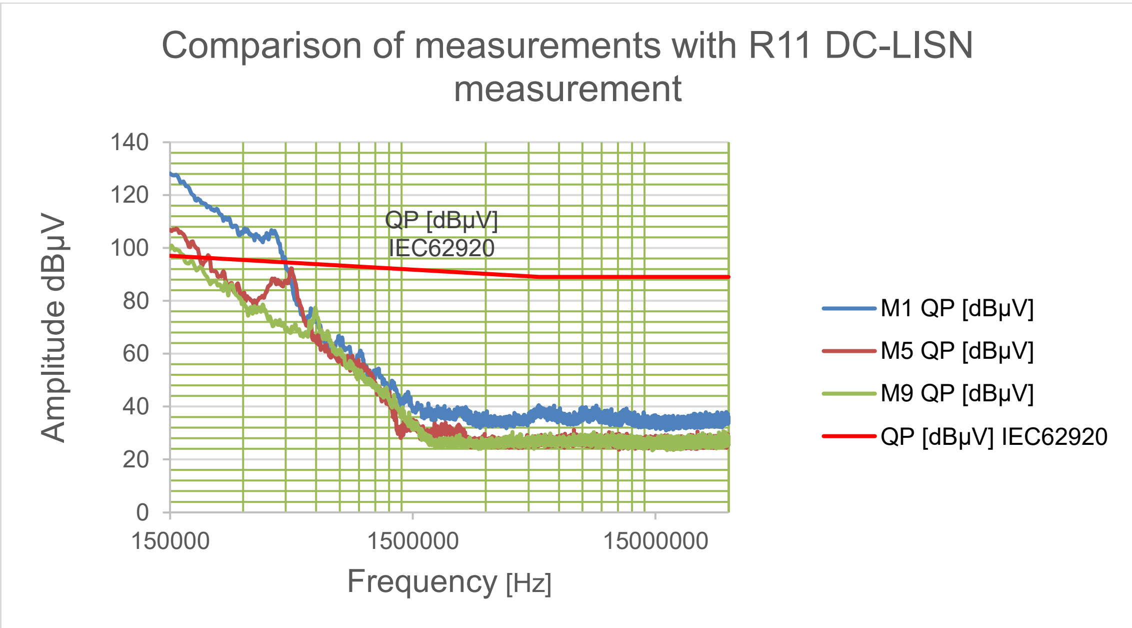

Figure 34 Quasi-peak values as a function of frequency

The measurement results of the two R11 setups that were presented in chapter 5.3.2 are presented below in figure 35 and 36. There is a comparison of measurements from common mode currents with 580 V_{dc} and with 799 V_{dc}. The difference between setups is that the EMI filter close to the EUT is either grounded to the laboratory conductive metal floor or to the EUT chassis.

The reason why the measurements of these setups is presented is that with both setups the measurement results of conducted emissions common mode would go under the limits of the standard IEC62920. This theoretically means that based on these measurements, the R11 model that was used in this thesis work could be used as a DC power source when measuring a Solar Pump DC application conducted emissions with voltages between 580 V_{dc} to 799 V_{dc}.

Comparison of measurement results between measurements M92 and M96 is shown in figure 35. Voltage level used in these measurements was 580 V_{dc}.

- M92 the EMI filter is grounded to the laboratory floor.
- M96 the EMI filter is grounded to the EUT chassis.
- IEC62920 limit class A rated power of ≤ 20 kVA is used as a measurement comparison in the graph.

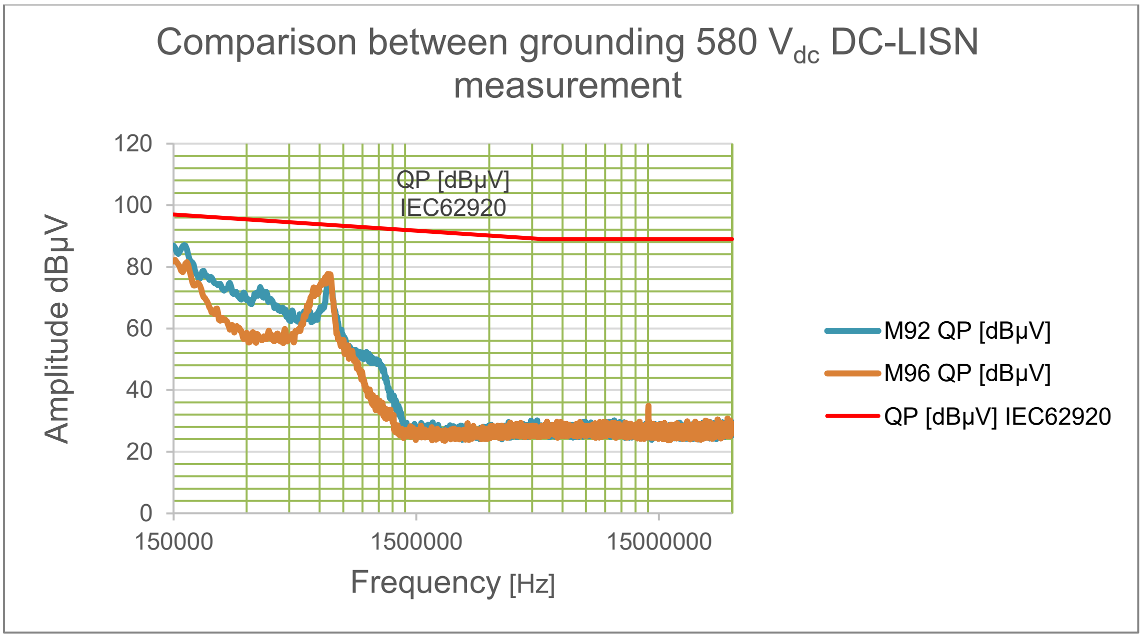

Figure 35 Quasi-peak values as a function of frequency with 580 V_{dc}

Comparison of measurement results between measurements M96 and M98 is shown in figure 36. Voltage level used in these measurements was 799 V_{dc}.

- M94 the EMI filter is grounded to the laboratory floor.
- M98 the EMI filter is grounded to the EUT chassis.
- IEC62920 limit class A rated power of ≤ 20 kVA is used as a measurement comparison in the graph.

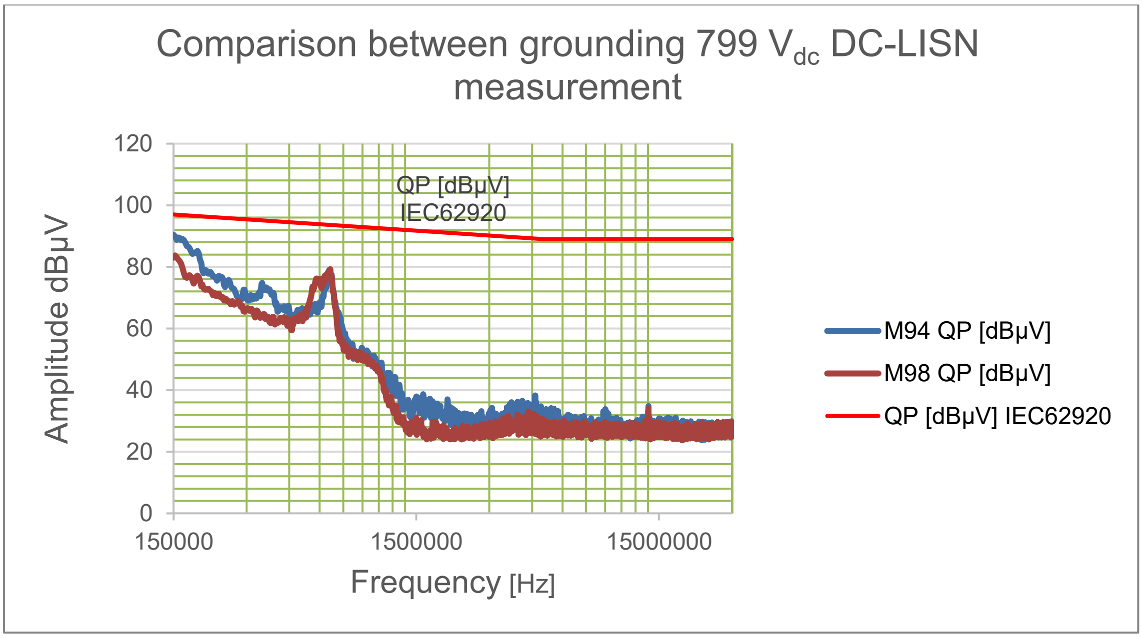

Figure 36 Quasi-peak values as a function of frequency with 799 V_{dc}

The maximum quasi-peak values from all the measurements presented in this thesis from the R11 is presented in table 5 below.

Table 5 Maximum quasi-peak values from R11 measurements

Measurement case	Quasi-peak maximum value between range of 0.15 – 30 MHz
M1	128.09 dBμV
M5	107.32 dBμV
M9	100.25 dBμV
M92	87.05 dBμV
M94	90.41 dBμV
M96	82.19 dBμV
M98	83.65 dBμV

6.3 Magna-Power

Comparison of measurements between voltage levels of 580 V_{dc} and 799 V_{dc} with Magna-power is shown in figure 37. Measurement M101 is with 580 V_{dc} and measurement M103 is with 799 V_{dc}. IEC62920 limit class A rated power of ≤ 20 kVA is used as a measurement comparison in the graph. Setup used in measurements is presented in chapter 5.3.3. The maximum quasi-peak values of the measurements M101 and M103 is presented in table 6.

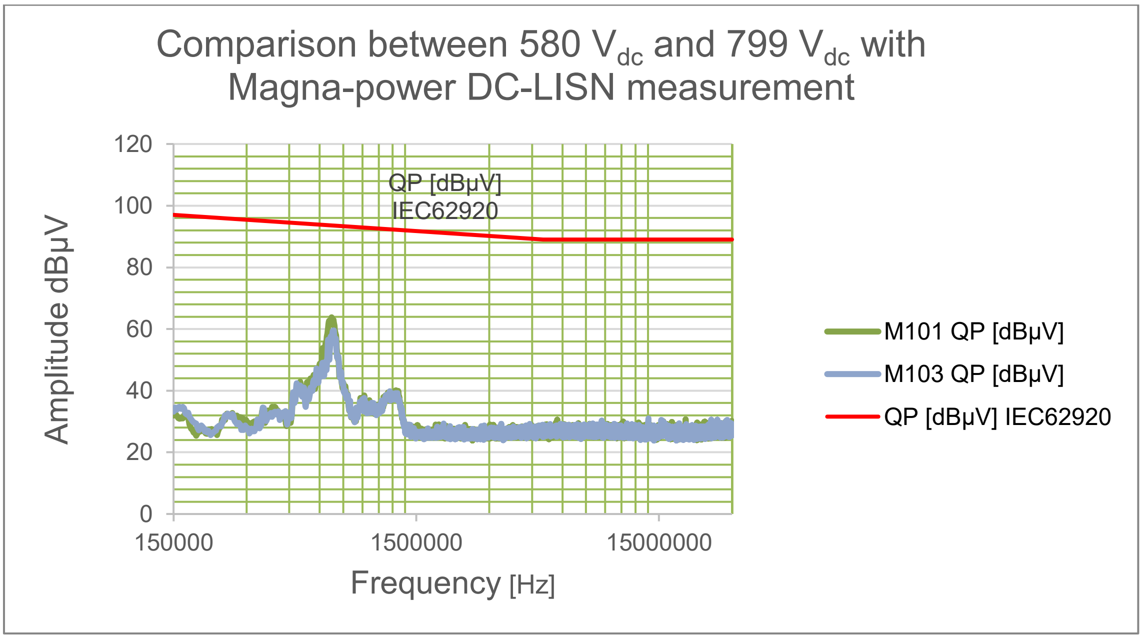

Figure 37 Quasi-peak values as a function of frequency with 580 V_{dc} and 799 V_{dc}

Table 6 Maximum quasi-peak values from Magna-power measurements

Measurement case	Quasi-peak maximum value between range of 0.15 – 30 MHz
M101	63.83 dBµV
M103	59.59 dBµV

7 Solar Pump Testing Against EMC Standards with Selected Power Source

Solar Pump was tested with multiple different types of measurements with Magna-Power as a DC power source. Solar Pump was also tested with Magna-power and AC grid power supply working simultaneously. The AC motor reference was set to 35 Hz in all measurements when the Solar pump application was modulating. 35 Hz frequency was chosen for the reason that it has been found to be the worst-case scenario when measuring the conducted emissions. Measurements presented below is with setup presented in chapter 5.3.3.

Measurements that are presented in figure 38 are common mode current measurements with the DC-LISN, Magna-power acting as a power source. The reference of 35 Hz is set to the motor with both measurements presented. Measurement M109 is with 580 V_{dc}, and it takes 0.8 A current from power source. Measurement M111 is with 799 V_{dc}, and it takes the current of 0.03 A from the power source. IEC62920 limit class A rated power of ≥ 20 kVA is used as a measurement comparison in the graph.

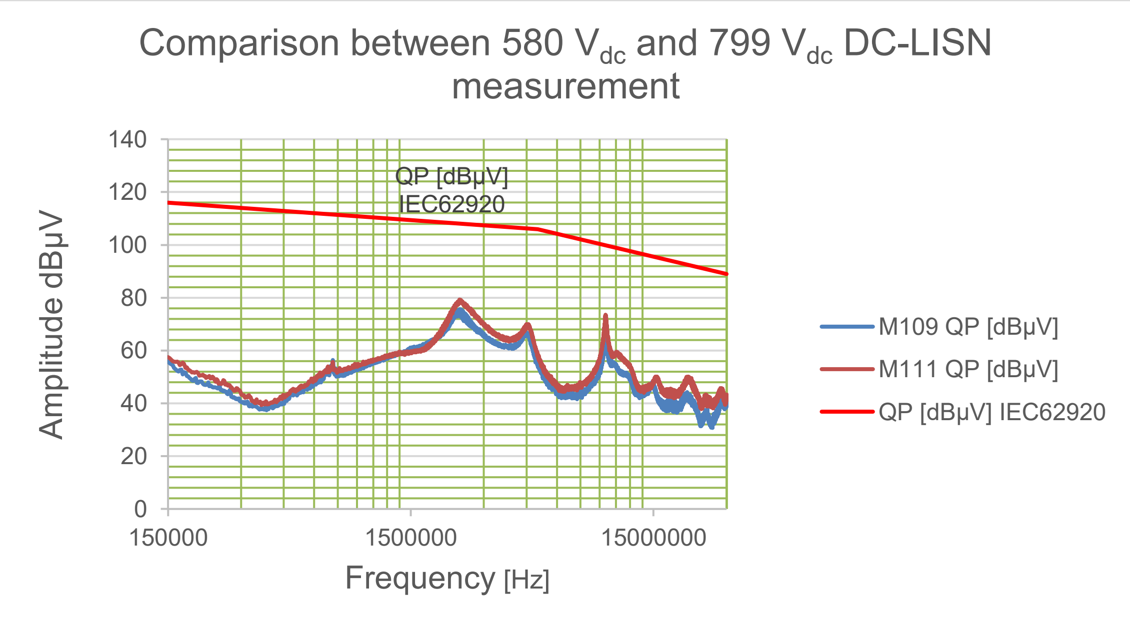

Figure 38 Common mode measurement with DC-LISN, ACQ80-22kW modulating

Comparison of the quasi-peak values between measurements M109 and M111 is presented in table 7 below. The only difference between measurements is the level of the supply voltage.

Table 7 Quasi-peak values from measurements M109 and M111

Measurement	M109	M111
Maximum quasi-peak value(dBµV)	75.67 dBµV	79.17 dBµV
Quasi-peak value(dBµV) 0.15 MHZ	55.89 dBµV	57.46 dBµV
Quasi-peak value(dBµV) 5 Mhz	54.52 dBµV	57.82 dBµV
Quasi-peak value(dBµV) 30 Mhz	41.11 dBµV	42.79 dBµV

Measurements that are presented in figure 39 are common mode current measurements with AC-LISN when DC- and AC power source are working simultaneously. Magna-power output voltage is set to 799 V_{dc}, and it takes 0.7 A current. AC grid power of 400 V is also connected to the ACQ80-22kW. Both power sources are feeding the device simultaneously. Measurements are taken with AC-LISN from phases L1, L2, and L3. Motor reference is 35 Hz and runs 1050 rpm. IEC62920 limit class A rated power of ≥ 20 kVA is used as a measurement comparison in the graph. Quasi-peak values from measurements M122, M123, and M124 are presented in table 8.

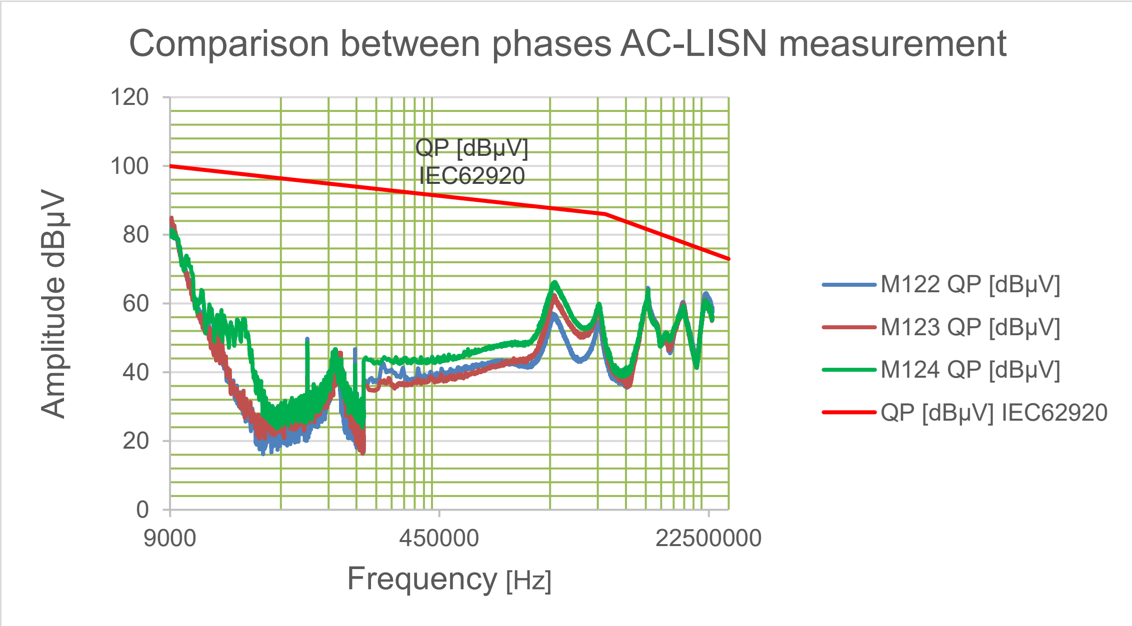

Figure 39 DC- and AC power simultaniously as power supply. Common mode measurement with AC-LISN, ACQ80-22kW modulating

Table 8 Quasi-peak values from measurements M122, M123, and M124

Phase	L1	L2	L3
Maximum quasi-peak value(dBµV)	83.29 dBµV	84.97 dBµV	81.36 dBµV
Quasi-peak value (dBµV) 9 kHZ	82.90 dBµV	84.29 dBµV	80.39 dBµV
Quasi-peak value (dBµV) 5 Mhz	44.79 dBµV	47.70 dBµV	48.67 dBµV
Quasi-peak value (dBµV) 30 Mhz	31.35 dBµV	26.76 dBµV	30.22 dBµV

Measurements shown in figure 40 are common mode current measurements with DC-LISN when DC- and AC power source are working simultaneously. The reference of 35 Hz is set to the motor with both measurements that are presented. Measurement M125 is with Magna-power output voltage of 799 V_{dc}, and it takes 0.7 A current from the power source. AC grid power of 400 V_{AC} is also connected to the ACQ80-22kW. Both power sources are feeding the device simultaneously. Measurement M127 is Magna-power output voltage of 618 V_{dc}, and it takes the current of 0.77 A from the power source. AC grid power of 400 V is also connected to the ACQ80-22kW. Both power sources are feeding the device simultaneously. IEC62920 limit class A rated power of ≥ 20 kVA is used as a measurement comparison in the graph. Specific voltage of 618 V_{dc} was selected according to the previous experiences during the EMC emission testing. 618 V_{dc} is a voltage level with this drive system when the device takes power from both AC- and DC power sources. Higher emission levels occur when the drive system takes power from both AC- and DC power sources at the same time. Quasi-peak values from measurements M125 and M127 are presented in table 9.

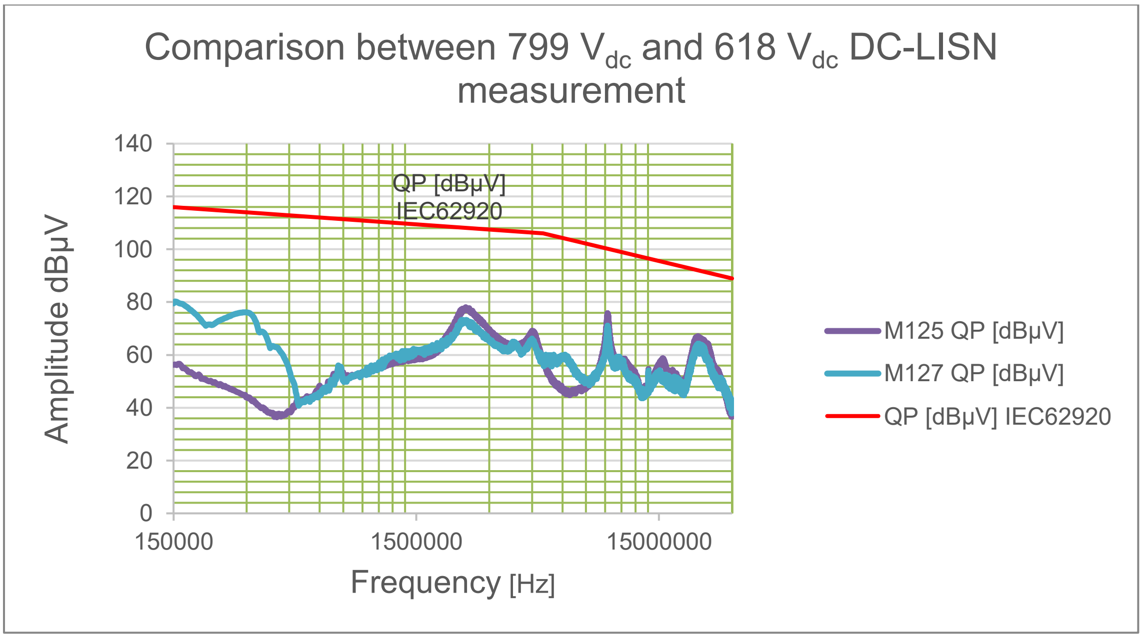

Figure 40 DC- and AC power simultaniously as power supply. Common mode measurement with DC-LISN, ACQ80-22kW modulating

Table 9 Quasi-peak values from measurements M125 and M127

Measurement	M125	M127
Maximum quasi-peak value(dBµV)	78.06 dBµV	80.22 dBµV
Quasi-peak value(dBµV) 0.15 MHZ	56.27 dBµV	79.54 dBµV
Quasi-peak value(dBµV) 5 Mhz	57.59 dBµV	59.69 dBµV
Quasi-peak value(dBµV) 30 Mhz	37.53 dBµV	40.49 dBµV

8 Conclusion

Several solutions for the solar pump DC power supply application were investigated. Main problem with power supply solutions is usually high conducted emission levels, which are exceeding the standard limits regardless of actual tested equipment. Numerous methods were used to solve these EMC problems and acceptable emission levels were achieved.

From the measurement results it can be concluded that R8i can be left out from the comparison between the EUT. It did not reach the limits of the standard IEC62920 in the measurements. R11's measurement results reached to the limits of the standard IEC62920. R11 could be an in-house solution, but there are multiple problems with it. R11 was tested as a DC power source after measurements were done. A suitable measurement setup was built that reached the limits of the standard IEC62920. The chosen R11 setup was used to power small ACQ80-11kW apparatus. After the modulation was started by giving the DC voltage reference of 580 V_{dc} with R11, ACQ80 gave an error message of an over voltage. The short modulation with R11 to power the ACQ80 was enough to destroy the device. The reason for breakage of the drive is under investigation, but there are some probable reasons for the unexpected behavior. These could be high voltage spikes on the lower frequencies or common mode voltages in the test system, which were "pumping" the DC link voltage too high and caused explosion of the DC link capacitors. Also, the measurement range with R11 is much narrower than with Magna-Power.

Magna-power is a superior choice between the EUT in this thesis work. Magna-power has the lowest “noise” levels in the measurements. R11 has multiple problems, and the practicality would be in favor for the Magna-power just for its small size and simplicity. Table 10 shows maximum quasi-peak values from measurements between all the EUT in this thesis work. The measurement results that are presented in the table 10 are the best-case scenario results with the devices.

Table 10 Comparison of the EUT’s measured maximum quasi-peak values in best-case scenario

EUT	R8i	R11	Magna-power
Maximum quasi-peak value(dBµV)	99.82 dBµV	83.65 dBµV	63.84 dBµV
Quasi-peak value 0.15 Mhz	99.82 dBµV	83.00 dBµV	33.23 dBµV
Quasi-peak value 5 Mhz	38.27 dBµV	27.03 dBµV	26.98 dBµV
Quasi-peak value 30 Mhz	26.78 dBµV	27.45 dBµV	27.40 dBµV

Due to the other limitation with drive as a DC power source it was found that commercially available special DC power supply suited best for the solar pump EMC testing. These reasons were low conducted emission levels, compact size, and user experience (very easy to operate) compared to the drive as a DC power supply. Future research will include the feasibility study of using drive as DC power source for the high-power solar pump applications.

References

1 VFDs. What is VFD, how it works? – VFD working principle [Internet]. 2022 [cited 10 January 2022]. Available from: http://www.vfds.org/what-is-vfd-how-it-works-964803.html.

2 Electrical Terminology. Variable frequency drive (VFD): Working principle, Function [Internet]. 2021 [cited 10 January 2022]. Available from: http://www.electricalterminology.com/what-is-variable-frequency-drive/.

3 Tang J. Oriental Motor. Speed Control Basics: VFD or Triac for AC Induction Motors [Internet]? 2021 [cited 10 January 2022]. Available from: https://blog.orientalmotor.com/speed-control-basics-speed-control-methods-of-ac-induction-motors.

4 ABB. Solar pump drive [Internet]. 2022 [cited 19 February 2022]. Available from: https://new.abb.com/drives/low-voltage-ac/industry-specific-drives/acq80-solar-pump.

5 Sines Export. Solar pump application example from ABB [Internet]. 2022 [cited 21 March 2022]. Available from: https://www.sines-export.com/solar-pump-inverter/abb-acs355.html.

6 Engineer Wagar. Mechanical Boost. What is Solar Water Pump? How does Solar System work [Internet]? 2020 [cited 24 February 2022]. Available from: https://mechanicalboost.com/solar-water-pump/.

7 ManualsLib. ABB. ACQ80-04 drives Hardware manual [Internet]. 2022 [cited 19 February 2022]. Available from: https://www.manualslib.com/products/Abb-Acq80-04-04kw0-4-10562454.html.

8 Tech Web. Switching noise – EMC, what is EMC [Internet]? 2018 [cited 7 February 2022]. Available from: https://techweb.rohm.com/knowledge/emc/s-emc/01-s-emc/6347.

9 AstrodyneTDI. Conducted EMI vs Radiated EMI — What's the difference [Internet]? 2022 [cited 18 February 2022]. Available from: https://www.astrodynetdi.com/blog/conducted-emi-vs.-radiated-emi-whats-the-difference.

10 ScienceDirect. Conducted Emissions [Internet]. 2022 [cited 14 February 2022]. Available from: https://www.sciencedirect.com/topics/engineering/conducted-emission.

11 Henry W. Tech Web Switching noise – EMC, Differential (Normal) Mode Noise vs Common Mode Noise – Causes and Measures [Internet]. 2018 [cited 7 February 2022]. Available from: https://techweb.rohm.com/knowledge/emc/s-emc/01-s-emc/6899.

12 International standard, IEC 62920 Edition 1.1 [pdf].

13 International standard, CISPR 11 Edition 6.2 [pdf].

14 Chen W, Zhi N, Ji J.P, Yang X, Zhang X. ResearchGate. A layout method for passive EMI filter [Internet]. 2017 [cited 22 February 2022]. Available from: https://www.researchgate.net/publication/321356818_A_layout_method_of_passive_EMI_filter.

15 Berman Mel. Electronic Products All about Emi filters [Internet]. 2008 [cited 7 February 2022]. Available from: https://www.electronicproducts.com/all-about-emi-filters/#.

16 Radius power. What is an EMI/RFI filter [Internet]? 2022 [cited 14 February 2022]. Available from: http://www.radiuspower.com/emi-filters.

17 Apogeeweb. Page article. EMI Filter Basics [Internet]. 2019 [cited 17 February 2022]. Available from: https://www.apogeeweb.net/article/1004.html.

18 Passive Components. Active vs Passive EMI filtering [Internet]. 2021 [cited 24 February 2022]. Available from: https://passive-components.eu/active-vs-passive-emi-filtering/.

19 AstrodyneTDI. EMI Shielding vs Filtering [Internet]. 2022 [cited 28 February 2022]. Available from: https://www.astrodynetdi.com/blog/emi-shielding-vs-filtering.

20 Cherry Clough Consultants. EMC, systems & installations, 2000, Part 2, Installations [Internet]. 2007 [cited 1 March 2022]. Available from: https://www.emcstandards.co.uk/files/emc_systems__installations_2000_part_2_installations.pdf.

21 Testequity. What is LISN (Line Impedance Stabilisation Network) [Internet]? 2018 [cited 4 March 2022]. Available from: https://mcs-testequipment.com/news/what-is-a-lisn-and-why-are-there-so-many-different-types.

22 Schawarzbeck. Schawarzbeck Mess Electronic, PVDC 8301 [Internet]. 2022 [cited 4 March 2022]. Available from: http://www.schwarzbeck.de/en/lisn-line-impedance-stabilisation-networks/special-lisn/471-pvdc-8301-dc-lisn.html.

23 Schawarzbeck. Schawarzbeck Mess Electronic, PVDC 8301 Datasheet [Internet]. 2022 [cited 4 March 2022]. Available from: http://schwarzbeck.de/Datenblatt/k8301.pdf.

24 Rohde & Schwarz. Rohde & Schwarz, ESPR3 EMI Test Receiver [Internet]. 2022 [cited 4 March 2022]. Available from: https://www.testwall.com/product/rohde-schwarz-esrp3-2/.

25 Tektronix. Tektronix DPO 4000 series data sheet [Internet]. 2022 [cited 4 March 2022]. Available from: https://www.testequipmenthq.com/datasheets/TEKTRONIX-DPO4104-Datasheet.pdf.

26 Rohde & Schwarz. ESH3-Z2 Pulse limiter [Internet]. 2022 [cited 4 March 2022]. Available from: https://www.rohde-schwarz.com/au/products/test-and-measurement/additional-accessories/rs-esh3-z2-pulse-limiter_63493-9091.html.

27 Schaffner. EMC/EMI Filter FN2200 Data sheet [Internet]. 2022 [cited 14 March 2022]. Available from: https://www.schaffner.com/product-storage/datasheets/fn2200/.

28 ABB. ACS880-104 IGBT supply units. Hardware manual [Internet]. 2022 [cited 24 April 2022]. Available from: https://library.e.abb.com/public/f52df72744e54e2ebf5fcaf1edd667c5/EN_ACS880-204_HW_J_A4.pdf.

29 ABB. ACS880-34 drive modules. Hardware manual [Internet]. 2022 [cited 24 April 2022]. Available from: https://library.e.abb.com/public/1f516945b4c348a79aa12f63e0a91c6e/EN_ACS880-34_HW_D_A4.pdf.